UNCLASSIFIED

AD NUMBER

AD069089

NEW LIMITATION CHANGE

TO

Approved for public release, distribution unlimited

FROM

Distribution authorized to U.S. Gov't. agencies and their contractors; Administrative/Operational Use; MAY 1955. Other requests shall be referred to Office of Naval Research, Arlington, VA 22203.

AUTHORITY

ONR memo., 1 Aug 1967

THIS PAGE IS UNCLASSIFIED

69089

Armed Services Technical Information Agency

Reproduced by
DOCUMENT SERVICE CENTER
KNOTT BUILDING, DAYTON, 2, OHIO

UNCLASSIFIED

Office of Naval Research

Contract N5ORI-76 • Task Order No.1 • NR-372-012

IMPEDANCE OF THIN WIRE LOOP ANTENNA

By

James E. Storer

May 1, 1955

Technical Report No. 212

Cruft Laboratory
Harvard University
Cambridge, Massachusetts

TR212

Office of Naval Research

Contract N5ori-76

Task Order No. 1

NR-372-012

Technical Report

on

Impedance of Thin Wire Loop Antennas

James E. Storer

May 1, 1955

The research reported in this document was made possible through support extended Cruft Laboratory, Harvard University, jointly by the Navy Department (Office of Naval Research), the Signal Corps of the U. S. Army and the U. S. Air Force, under ONR Contract N5ori-76, T.O. 1.

Technical Report No. 212

Cruft Laboratory

Harvard University

Cambridge, Massachusetts

TR212

Abstract

The Hallén integral equation for the current and impedance of a thin wire loop antenna is solved using a Fourier Series. Extensive tables of theoretical loop antenna impedances are presented which (for the one case tested) are in satisfactory agreement with experiment. Some graphical results are also given which facilitate the evaluation of the current distribution.

TR212

Impedance of Thin Wire Loop Antennas

by

James E. Storer

Cruft Laboratory, Harvard University

I

Introduction

The thin wire loop is one of the first antennas to receive theoretical consideration, having been discussed by Pocklington [1] in 1897. Pocklington treated a closed loop excited by a plane wave; he obtained an exact solution for the current on the loop in the form of a Fourier series. More recently, Hallén [2] considered a driven loop and obtained a solution, again in the form of a Fourier series, for the current and the impedance. However, Hallén pointed out that the coefficients of this series contained a singularity which made the series only quasiconvergent and hence useful only for loops small in comparison to a wavelength. Moreover, the individual terms were complicated and their evaluation and a summation involved a somewhat difficult numerical task.

More recently, in an effort to obtain numerical results, other authors have dealt with the problem using approximation methods. Chang [3], for example, applied the Hallén-King-Middleton expansion; Schelkunoff [4] has used a guided-mode approximation; and the author (unpublished) has used a variational approach. All of these approximation methods have one feature in common; they yield results which are in good agreement qualitatively with experiment, but poor agreement quantitatively.* The reason for this can be explained by noting that all the approximation methods require some assumption as to the current distribution around the loop. The most common

------

*It is quite possible that all of these methods, particularly Chang's, could be made to yield better results by going to higher degrees of approximation; the resulting numerical labor, however, is likely to be prohibitive.

assumption made is that the current distribution approximates a sinusoidal distribution. As will be shown subsequently, the sinusoidal assumption is not satisfactory, particularly for the current near the driving point of the antenna.

In the present paper the rigorous Fourier series solution obtained by Hallén is reexamined, and modified so that the convergence difficulties encountered by Hallén are avoided. Extensive numerical results are presented in Appendix II for the impedances of loops for varying wire sizes and circumferences up to two and one-half wavelengths. Appendix III presents some curves which aid in the computation of field patterns and current distributions. For an antenna having a particular wire size, some experimentally measured impedances are presented which agree well with theory.

II

Fourier Series Solution for the Current Distribution

Integral equations for the current distribution on thin-wire antenna structures are readily obtained by expressing the electric field as a function of the current, through Helmholtz integrals, and then equating the total electric field to zero along the wire surface. Following this procedure, with harmonic time dependence of the form $e^{+j\omega t}$, and with coordinate system and dimensions as indicated in Fig. 1.1, the integral equation for the circular loop antenna

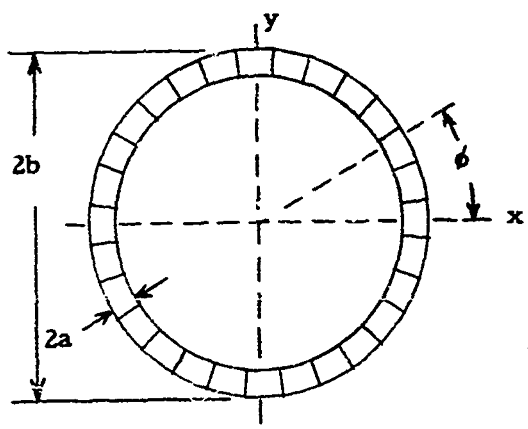

Figure 1.1

can be written as

$$V\delta(\phi) = \frac{j\zeta_0}{4\pi} \int_{-\pi}^{\pi} K(\phi-\phi')I(\phi')d\phi' \tag{1}$$

where $I(\phi)$ is the total current at ϕ on the loop; V is the voltage of the slice generator exciting the loop at $\phi = 0$; $\delta(\phi)$ is the Dirac delta-function; and $k = \omega/c = 2\pi/\lambda$; $\zeta_0 = \sqrt{\frac{\mu_0}{\epsilon_0}} = 120\pi$ ohms. The kernel of the integral equation, (1) is given explicitly by

$$K(\phi-\phi') = \left\{ kb\cos(\phi-\phi') + \frac{1}{kb}\frac{\partial^2}{\partial\phi^2} \right\} \frac{e^{-jkbR(\phi-\phi')}}{R(\phi-\phi')} \tag{2a}$$

$$R(\phi-\phi') = \left[4\sin^2\left(\frac{\phi-\phi'}{2}\right) + a^2/b^2 \right]^{\frac{1}{2}} \tag{2b}$$

where a is the radius of the wire and b is the radius of the loop.

The thin-wire assumption, which provides the basis for obtaining this one-dimensional current equation, can be expressed explicitly as $a^2 \ll b^2$, $k^2a^2 \ll 1$. The resulting solution cannot be more accurate than the order of these approximations.

Since $\frac{1}{R(\phi-\phi')} e^{-jkbR(\phi-\phi')}$ is a bounded, periodic function of ϕ, it can be expanded into a Fourier series, i.e.,

$$\frac{1}{R(\phi-\phi')} e^{-jkbR(\phi-\phi')} = \sum_{-\infty}^{\infty} K_n e^{-jn(\phi-\phi')} \tag{3}$$

$$K_n = K_{-n} = \frac{1}{2\pi} \int_{-\pi}^{\pi} \frac{e^{-jkbR(\phi)}}{R(\phi)} e^{-jn\phi} d\phi \tag{4}$$

Using (3) together with (2), it is seen that

$$K(\phi-\phi') = \sum_{-\infty}^{\infty} a_n e^{jn(\phi-\phi')}, \tag{5}$$

where

$$a_n = a_{-n} = kb\left\{\frac{K_{n+1}+K_{n-1}}{2}\right\} - \frac{n^2}{kb}K_n \qquad (6)$$

Inserting expression (5) into integral equation (1) yields

$$V\delta(\phi) = \frac{j\zeta_o}{4\pi}\sum_{-\infty}^{\infty} a_n \int_{-\pi}^{\pi} e^{jn(\phi-\phi')} I(\phi')d\phi' \qquad (7)$$

After expanding $I(\phi)$ into a Fourier series,

$$I(\phi) = \sum_{-\infty}^{\infty} I_n e^{jn\phi}; \quad I_n = \frac{1}{2\pi}\int_{-\pi}^{\pi} I(\phi)e^{-jn\phi}d\phi \qquad (8)$$

it can be seen that (7) reduces to

$$V\delta(\phi) = \frac{j\zeta_o}{2}\sum_{-\infty}^{\infty} a_n I_n e^{jn\phi}$$

Hence

$$I_n = \frac{1}{j\pi\zeta_o a_n}\int_{-\pi}^{\pi} e^{-jn\phi} V\delta(\phi)d\phi = \frac{V}{j\pi\zeta_o a_n}$$

Inserting this result into equation (8) yields

$$I(\phi) = \frac{V}{j\pi\zeta_o}\sum_{-\infty}^{\infty}\frac{e^{jn\phi}}{a_n} = \frac{V}{j\pi\zeta_o}\left\{\frac{1}{a_o} + 2\sum_{1}^{\infty}\frac{\cos n\phi}{a_n}\right\} (9)$$

From this, the impedance of the antenna, Z, is found to be

$$Z = \frac{V}{I(o)} = j\pi\zeta_o\left\{\frac{1}{a_o} + 2\sum_{1}^{\infty}\frac{1}{a_n}\right\}^{-1} \qquad (10)$$

These results, (9) and (10), which were obtained by Hallén, constitute a formal solution of the loop antenna. From them the transmitting pattern and by reciprocity the receiving pattern can be obtained. However, in order to make them useful, some way must be found to evaluate the series numerically.

It can be shown that these equations, (9) and (10), are in agreement with the theory of small loops. Using equation (4), and the explicit evaluation of K_n given in Appendix I, it is readily shown that for loops small in comparison to the wavelength the current is nearly a constant, independent of ϕ and

$$kb \ll 1, \quad Z \cong j\pi\zeta_0 a_0 = j\pi\zeta_0 kbK_1$$
$$\cong \frac{\pi\zeta_0}{6} k^4b^4 + j\pi\zeta_0 kb\left[\ln\frac{8b}{a} - 2\right]$$

This is the usual formula for the resistance and reactance of a small loop.

III

The Fourier Series

It is apparent from the preceding derivation that the usefulness of this method of solution depends on the evaluation of the series

$$I(\phi) = \frac{jV}{\pi\zeta_0}\left\{\frac{1}{a_0} + 2\sum_{1}^{\infty}\frac{\cos n\phi}{a_n}\right\}. \tag{11}$$

Hallén proved that, for large n, the coefficients approach asymptotically the value

$$a_n \sim -\frac{n^2}{\pi kb}\left\{\ln\frac{2b}{a} - \gamma - \ln n\right\},$$

where γ (= .5772) is Euler's constant. It is apparent that a_n becomes extremely small for values of n such that

$$n \cong n_0 = \frac{2b}{a}\, e^{-\gamma}$$

Hence the series (11) has a "singularity" near $n \cong n_0$. From this fact Hallén concluded that the series (11) could only be used in an "asymptotic" fashion, i.e., it must converge satisfactorily by $n \cong \frac{n_0}{2}$ since after this the value of the individual terms begin increasing in magnitude. This restriction meant that the series solution (11) was only useful for kb small or b/a very large. Even with this limitation the summation of $n_0/2$ terms of this series in a formidable task and, at best, yields relatively inaccurate results because of the "singularity."

It must be remembered at this point that current is both bounded and continuous (for physical reasons) and hence the series (11) must converge. Adopting this point of view, the problem then becomes one of treating Hallen's "singularity" in a more rigorous fashion.

A derivation of the value of a_n is given in Appendix A, which is essentially identical to that of Hallen's, but which includes the dominant complex term as well. The result for large n is

$$a_n \sim \frac{1}{\pi}\left(kb - \frac{n^2}{kb}\right)\left(\ln n_o - \ln n - j\,\frac{(kb)^{2n+1}}{\Gamma(2n+2)}\right) \qquad \begin{matrix} n > kb \\ n \gg 1 \end{matrix} ,$$

where $n_o = \frac{2b}{a} e^{-\gamma}$.

It is apparent that the inclusion of the rather negligible complex term in (12) cannot alter significantly the sum of the resulting series. However, with its inclusion a_n is never equal to zero. This fact will be used subsequently to permit a replacement of the series by an integral.

The following work will be restricted to loops in which kb $\leq$ 2.5 — i.e., the circumference of the loop is less than two-and-a-half wavelengths.* Almost all loop antennas of practical interest are contained in this range. The series (11) can then be written in the form

$$I(\phi) = \frac{V}{j\pi \zeta_o}\left\{\frac{1}{a_o} + 2\sum_{1}^{4}{}' \frac{\cos n\phi}{a_n} + \psi(\phi)\right\} , \qquad (12)$$

where

$$\psi(\phi) = 2\sum_{5}^{\infty}{}' \frac{\cos n\phi}{a_n} . \qquad (13)$$

The procedure to be used will sum the first five terms of the series explicitly, and replace the remainder of series $\psi(\phi)$ by an integral.

Now, it can be shown by an insertion of numerical values that for

- - - - - - -

*The derivation can readily be modified to include values of kb larger than 2.5 if desired.

$kb \leqq 2.5$ and $n \geqq 5$, the value of a_n differs negligibly from the asymptotic value given by (12). Hence, to an excellent approximation,

$$\psi(\theta) = -2\pi kb \int_{5}^{\infty} \frac{\cos n\phi}{(n^2 - k^2b^2)[\ln n_o - \ln n - j(kb)^{2n+1}/\Gamma(2n+2)]} . \quad (14)$$

The series (14) will now be replaced by an integral. The particular formula to be used is

$$\sum_{N}^{\infty} a_n = \int_{N-\frac{1}{2}}^{\infty} a_x\,dx + \sum_{o}^{\infty} c_n \left[\frac{d^{2n+1}}{dx^{2n+1}} a_x\right]_{x=N-\frac{1}{2}} , \quad (15)$$

$$\text{where } c_o = 1/24, c_1 = -\frac{7}{2^4 \cdot 360} , \text{ etc.}$$

This result, (15), is valid provided a_n is an analytic function of n in a region which includes the real axis for $n > N - \frac{1}{2} - \epsilon$. Results similar to (15) have been given by Gumowski [5] and others. It is essentially a modification of the Euler-McClaurin sum formula.

Using (15) in connection with (14) yields

$$\psi(\phi) = -2\pi kb \int_{4.5}^{\infty} \frac{\cos x\phi\,dx}{(x^2-k^2b^2)(\ln n_o - \ln x - j\frac{(kb)^{2x+1}}{\Gamma(2x+2)})} \quad (16)$$

$$\frac{2\pi kb}{24}\left[\frac{d}{dx}\frac{\cos x\phi}{(x^2-k^2b^2)(\ln n_o - \ln x - j\frac{(kb)^{2x+1}}{\Gamma(2x+2)})}\right]_{x=4.5} - \cdots$$

This replacement of the series (15) by the integral is possible only because of the complex term, which makes the argument an analytic function of x along the real axis. Since $kb \leq 2.5$, the first (and higher) derivative correction terms in (16) are small (less than 1%) compared to $\psi(\phi)$ and can be ignored, since $\psi(\phi)$ is at best a minor part of $I(\phi)$ in (14). Hence,

$$\psi(\phi) = -2\pi kb \int_{4.5}^{\infty} \frac{\cos x\phi\,dx}{x^2-k^2b^2)(\ln n_o - \ln x - j\frac{(kb)^{2x+1}}{\Gamma(2x+2)})} \quad (17)$$

Next, it can readily be shown that the complex term in the integral of (17) can also be ignored. This yields

$$\psi(\phi) = -2\pi kb \int_{4.5}^{\infty} \frac{\cos x\phi \, dx}{(x^2-k^2b^2)(\ln n_o - \ln x)} . \tag{18}$$

The integral in (18), which is to be interpreted in the "principal value" sense, can be rewritten as follows:

$$\psi(\phi) = \psi_1(\phi) + \psi_2(\phi) \tag{19a}$$

$$\psi_1(\phi) = -2\pi kb \int_{4.5}^{\infty} \frac{\cos x\phi}{\ln n_o - \ln x} \cdot \frac{dx}{x^2} \tag{19b}$$

$$\psi_2(\phi) = -2\pi kb \int_{4.5}^{\infty} \frac{\cos x\phi}{\ln n_o - \ln x} \cdot \frac{k^2b^2 dx}{x^2(x^2-k^2b^2)} \tag{19c}$$

Since n_o is quite large and $kb \leqq 2.5$, (19c) becomes, to a satisfactory approximation:

$$\psi_2(\phi) \cong \frac{-2\pi kb}{\ln n_o - \ln 4.5} \int_{4.5}^{\infty} \frac{k^2b^2 \cos x\phi}{x^2(x^2-k^2b^2)} \, dx$$

$$\cong \frac{-2\pi k^3b^3}{\ln(\frac{n_o}{4.5})} \int_{4.5}^{\infty} \frac{\cos x\phi}{x^4} \, dx$$

$$= -\frac{2\pi}{\ln(\frac{n_o}{4.5})} \cdot \left(\frac{kb}{4.5}\right)^3 J_2(\phi)$$

This integral, $J_2(\phi)$, can be evaluated explicitly in terms of sines, cosines, and integral sines.

Using these results, an explicit formula for the current distribution can be written as:

$$I(\phi) = \frac{V}{j\pi\zeta_o}\left\{\frac{1}{a_o} + 2\sum_{1}^{4}\frac{\cos n\phi}{a_n} - \frac{2\pi}{\ln\left(\frac{n_o}{4.5}\right)}\left[\left(\frac{kb}{4.5}\right)J_1(\phi) + \left(\frac{kb}{4.5}\right)^3 J_2(\phi)\right]\right\} \tag{20}$$

where

$$J_1(\phi) = \int_1^\infty \frac{\ln\left(\frac{n_o}{4.5}\right)}{\ln\left(\frac{n_o}{4.5}\right) - \ln x} \cdot \frac{\cos(4.5\phi)}{x^2}\,dx \tag{21a}$$

$$J_2(\phi) = \int_1^\infty \frac{\cos(4.5x\phi)}{x^4}\,dx \tag{21b}$$

$n_o = \frac{2b}{a}e^{-\gamma}$ and explicit formulas for the a_n are given in Appendix A.

Note that the $J_k(\phi)$ integrals have only appreciable values near $\phi = 0$. (An asymptotic formula for them, when $\phi > 1$, can readily be obtained.) They cannot be approximated satisfactorily by a sinusoid and are a partial explanation of why approximate methods of dealing with the loop antenna do not yield good quantitative results.

The formula for the impedance of the loop antenna becomes

$$Z = j\pi\zeta_o\left\{\frac{1}{a_o} + 2\sum_{1}^{4}\frac{1}{a_n} - \frac{2\pi}{\ln\left(\frac{n_o}{4.5}\right)}\left[\left(\frac{kb}{4.5}\right)J_1(o) + \left(\frac{kb}{4.5}\right)^3 J_2(o)\right]\right\}^{-1} \tag{22}$$

This result, in connection with Appendix A, forms the basis for the impedance tables presented in Appendix B. The quantities $J_k(o)$ are explicitly given by

$$J_1(o) = \frac{\ln\left(\frac{n_o}{4.5}\right)}{\left(\frac{n_o}{4.5}\right)} \int_{-\infty}^{\ln\left(\frac{n_o}{4.5}\right)} \frac{e^{+x}}{x}\,dx$$

$$J_2(o) = 1/3$$

IV

Results

The impedance of loop antennas for various values of b/a have been calculated using equation (22). As a parameter, the quantity

$$\Omega = 2\ln\frac{2\pi b}{a} \tag{23}$$

has been chosen. Note that $2\pi b/a = c/a$, where c is the circumference of the antenna. Hence (23) represents a definition analogous to that used for dipole antennas.

In Appendix B, values of the impedance are tabulated for $0 \leq kb \leq 2.5$ and $\Omega = 8, 9, 10, 11, 12$. They are also presented in graphical form. These impedances are useful for examining the operation of a loop antenna as a function of frequency. For laboratory purposes, however, it is sometimes convenient to have tables available appropriate to holding the frequency fixed and varying the size of the antenna. These are given at the end of Appendix B and have been obtained by interpolation from the earlier tables.

It is perhaps worth while to comment on some of the more obvious features of these loop antenna impedances. As can be seen, the first antiresonance, occurring when the circumference of the loop approximates a half-wavelength, is extremely sharp. This well-known effect is easily explained by noting that a sufficiently small loop resembles closely a short-circuited quarter-wavelength transmission line and has a correspondingly sharp antiresonance.

Of equal interest is the rapid disappearance of resonances as the circumference of the antenna increases. Thus, for $\Omega \leq 9$, a second resonance point does not even exist. If one compares these impedances with those for a dipole antenna, it is seen that the two are similar, both qualitatively and quantitatively, for $c > \lambda$. The prime difference is that the loop is essentially more capacitive (by about 130 ohms) than a dipole. This can be explained on the basis that charged surfaces are closer together on a loop than on a dipole. This shift in reactance level by 130 ohms permits the dipole to have several resonances and antiresonances, whereas, as noted previously, a moderately thick loop ($\Omega<9$) has essentially only one anti-resonance. The resistance curves for the loop and dipole are very similar, with the resistance minima having almost identical values.

It is interesting to compare these theoretical loop impedances with some experimentally measured ones. Miss Phyllis Kennedy of Cruft Laboratory has measured some loop impedances, using a half-loop over an image plane, and driven by a two wire line. The explicit configuration is indicated in Fig. 4.1a. One set of the admittances measured by Miss Kennedy appears in Fig. 4.1b together with the corresponding theoretical curves. The agreement between the theoretical and experimental curves is seen to be excellent. It is seen that the resistance peaks near resonance on the theoretical conductance curves are slightly higher than those on the experimental curve. This could have been anticipated as ohmic losses of the loop were not taken into account in the theoretical solution. The two susceptance curves differ by a slight additive amount throughout the entire range. This can readily be attributed to the so-called end coupling effect of the feeding line, which arises from the fact that the transmission-line excitation differs from the "slice generator" used in the theoretical model. King [6] has calculated this end effect for a dipole antenna. The dominant correction term is a negative capacitance in shunt with the antenna. Quite obviously, the end correction for a loop antenna should be similar, even to the order of magnitude. If such an approximate correction is made to the susceptance curve of Fig. 4.1b, this is changed in the right direction.

In Appendix C, values of the quantities $1/a_k$ and the functions $J_k(\phi)$ are presented graphically to facilitate evaluation of the current distribution using equations (20) and (21). To obtain an idea of the type of current distributions on loop antennas, some were calculated for the explicit case of $\Omega = 10$. Owing to the fact that the $J_k(\phi)$ were evaluated by numerical integration, there exists a slight discrepancy between $I(o)$ and the admittance. Since the admittance values are more accurate, they were used in place of $I(o)$.

One of the classic assumptions in antenna literature is that a small loop has a constant current distribution. To examine the validity of the assumption, the actual current distribution were calculated for $\Omega = 10$ and kb = .1, .2, .3, and .4. These appear in Fig. 4.2. It is apparent that for the smallest loop, kb = .1, the current varies in magnitude by about 5 and hence can be considered reasonably constant. For kb = .2, however, the variation is well over 10 %. On the basis of these results, one would be led to the conclusion that loops much larger than kb = . 2 cannot be considered small.

In order to obtain an idea of how the distribution of current varies as the size loop increased, values of it were calculated for $\Omega = 10$ and kb = .5, 1.0, 1.5, 2.0, and 2.5. These results appear in Fig. 4.3. Perhaps the most noticeable feature in these curves appears in the plots of magnitude and phase for the larger values kb. For values of $\phi < 90^{\circ}$, it is apparent that the current distribution is beginning to approximate a traveling wave, in the sense that variations in the magnitude have been reduced and the phase is becoming linear. This is in agreement with the observation made in connection with the impedances, namely, that for larger kb the magnitude of the variation of the resistance is reduced.

V

Acknowledgements

The author wishes to thank Professor R.W.P. King of Harvard University for his help and encouragement with this research, Miss Phyllis Kennedy for making her measurements available; and to Mr. Leon Levy, who performed the numerical computations.

The author also wishes to acknowledge the financial support he received from the Atomic Energy Commission as a Fellow during the early phase of this research, and during the latter part, under the sponsorship of the Office of Naval Research, the Signal Corps of the U.S. Army, and the U. S. Air Force (Contract N5ori-76).

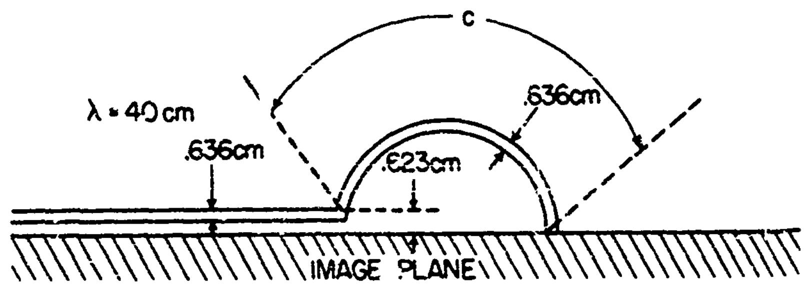

FIG. 4.1a EXPERIMENTAL DIMENSIONS

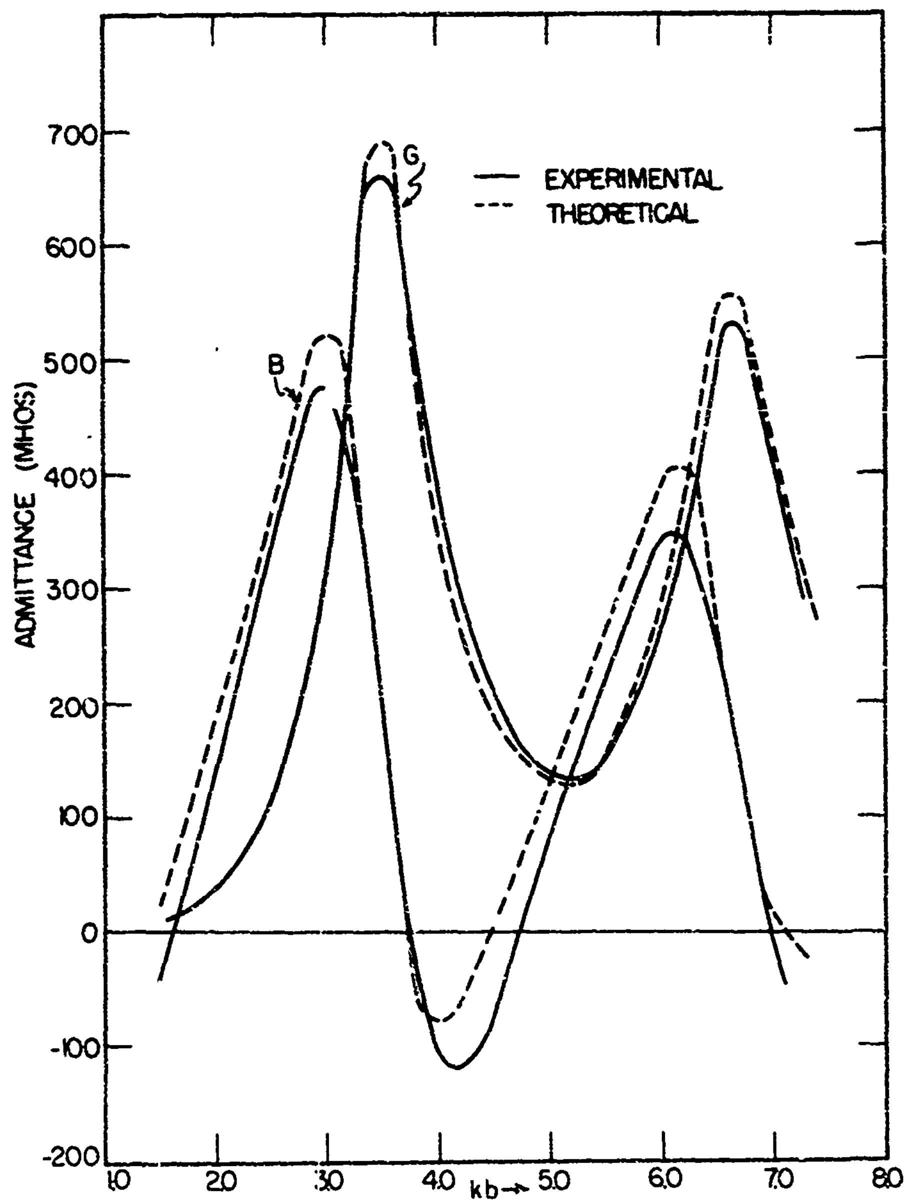

FIG. 4.1b

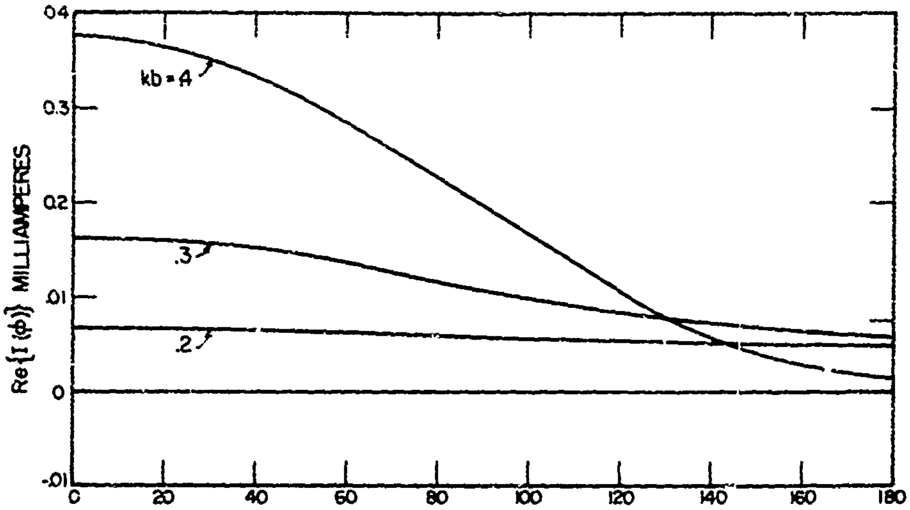

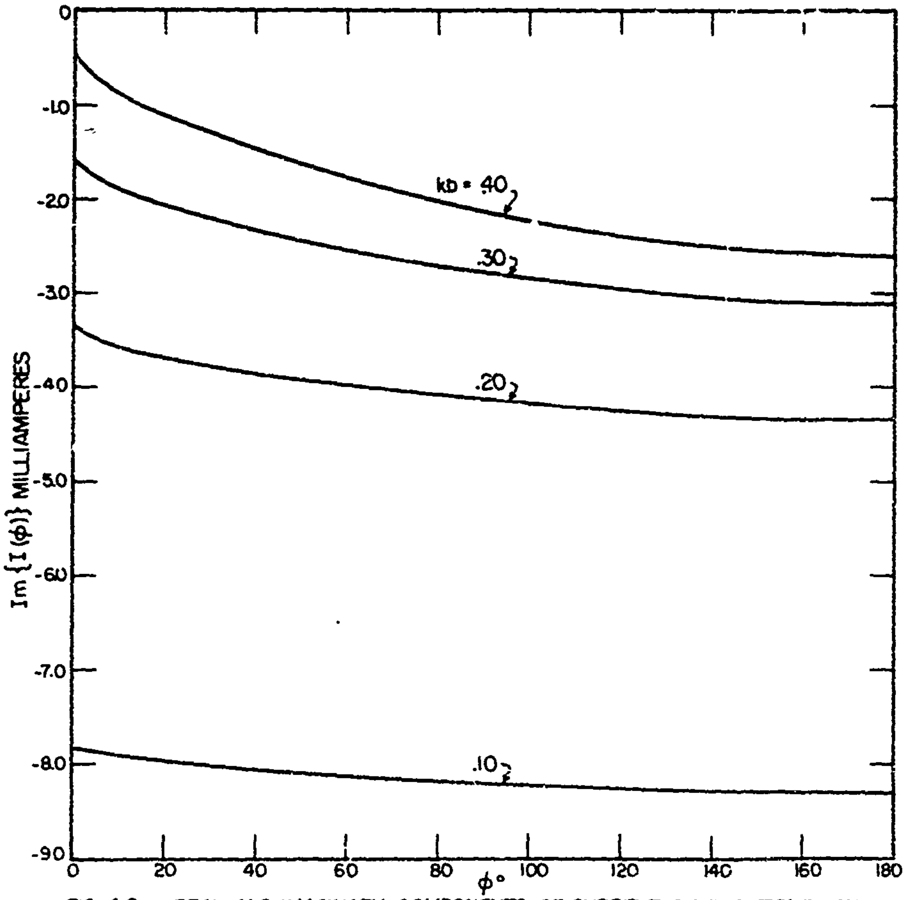

FIG 4.2a REAL AND IMAGINARY COMPONENTS OF CURRENT DISTRIBUTIONS ON SMALL LOOP ANTENNAE

$\Omega = 2\ln(2\pi b/a) = 10$

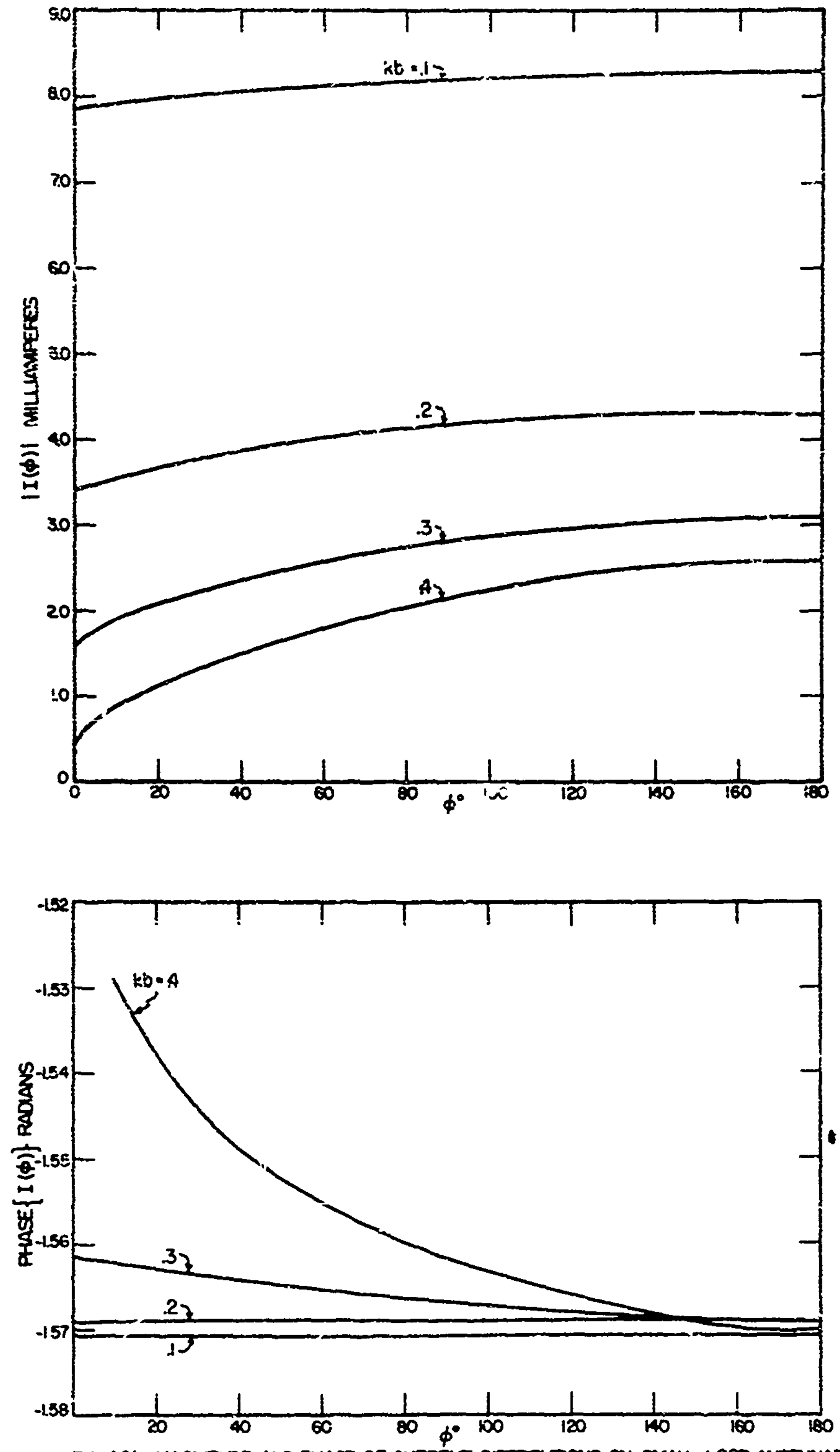

FIG. 4.2b MAGNITUDE AND PHASE OF CURRENT DISTRIBUTIONS ON SMALL LOOP ANTENNAE

$\Omega = 2\ln(2\pi b/a) = 10$

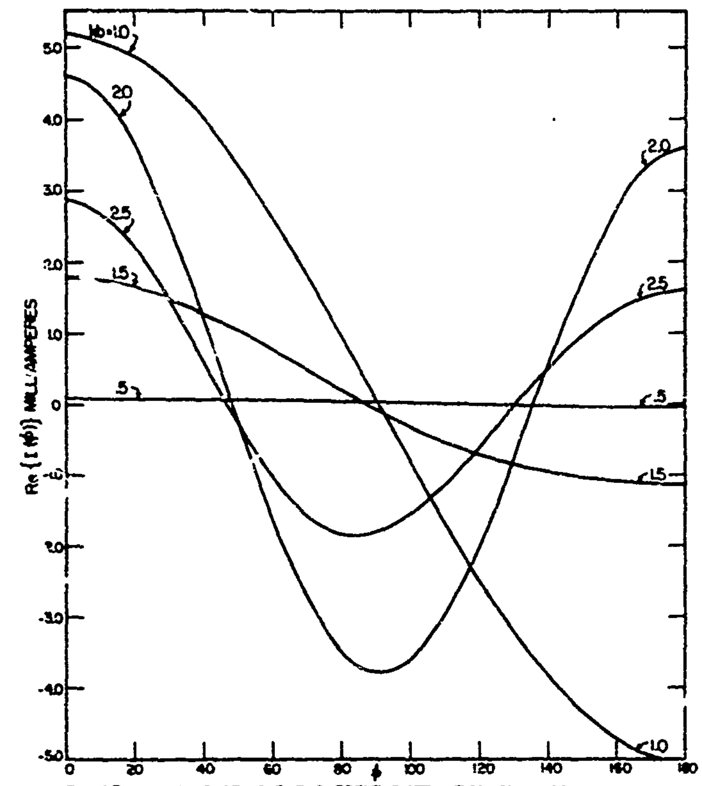

FIG. 4.3a REAL PART OF THE CURRENT DISTRIBUTION ON LOOP ANTENNAE
$\Omega = 2\ln(2\pi b/a) = 10$

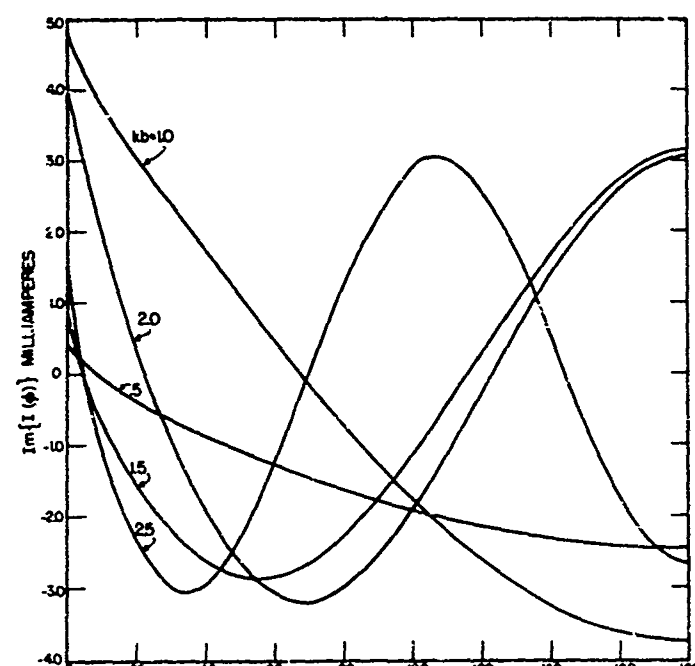

FIG. 4.3b IMAGINARY COMPONENT OF CURRENT DISTRIBUTION ON LOOP ANTENNAE
$\Omega = 2\ln(2\pi b/a) = 10$

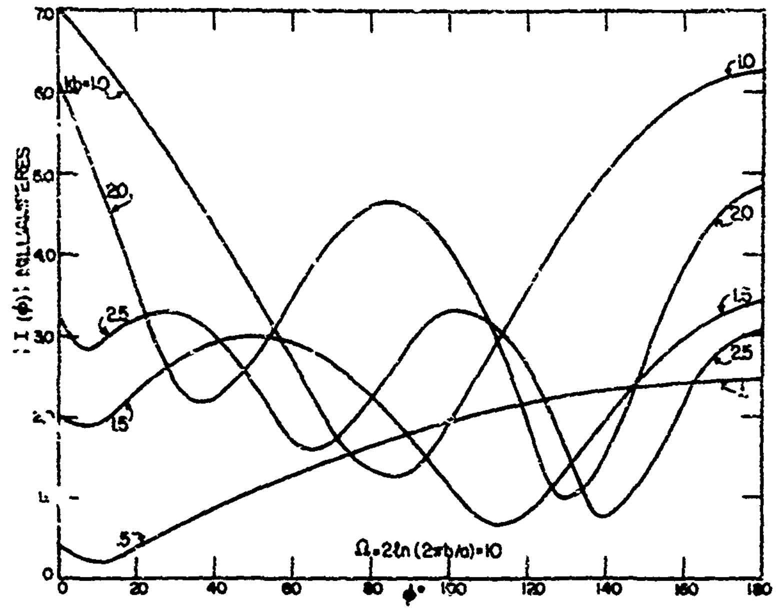

FIG. 4.3c MAGNITUDE OF CURRENT DISTRIBUTION ON LOOP ANTENNAE

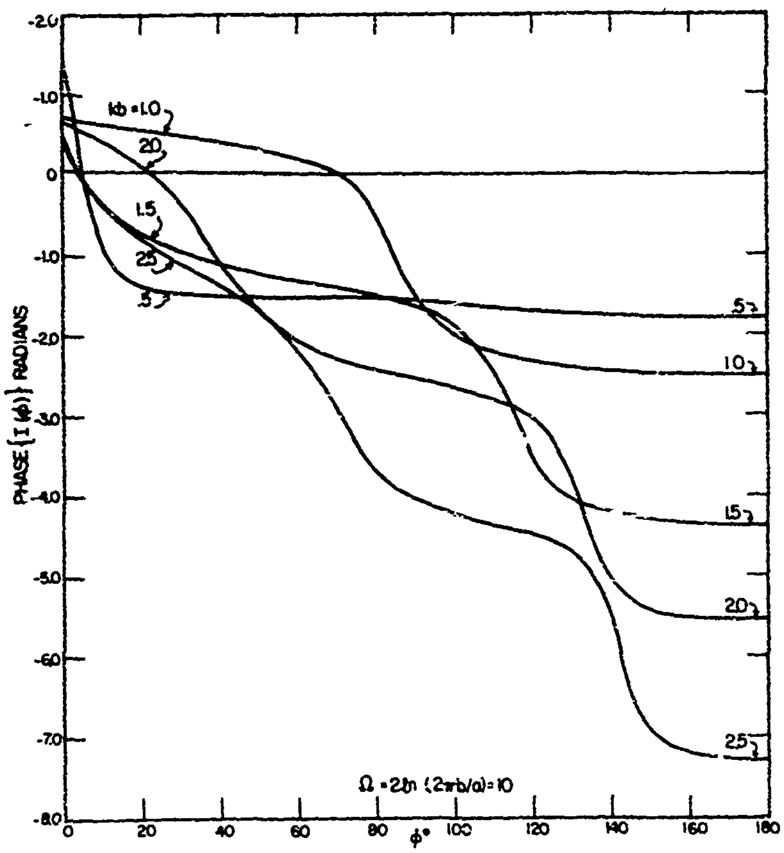

FIG. 4.3d PHASE OF CURRENT DISTRIBUTION ON LOOP ANTENNAE

References

1. H. C. Pocklington, Proc. Cambridge Phil. Soc. 9, 324 (1897).

2. E. Hallén, Nova Acta Reg. Soc. Uppsala, Ser. IV, vol. II, no. 4, November, 1938.

3. Tung Chang, Technical Report No. 16, Cruft Laboratory, Harvard University.

4. S. A. [illegible]unoff and H. T. Friis, Antenna Theory and Practice, Sect. 13.12; John Wiley, New York, 1952.

5. I. Gumowski, "Summation of Slowly Converging Series," J. Appl. Phys. 24, 1068 (1953).

6. R. King, "Theory of Antennas Driven from Two-Wire Line," J. Appl. Phys. 20, 832 (1949).

Appendix A

Evaluation of K_n

From (4) it is seen that

$$A_n = K_{n+1} - K_n = \frac{1}{2\pi}\int_0^{2\pi} \frac{e^{-jkbR(\phi)}}{R(\phi)}\left[e^{j(n+1)\phi} - e^{jn\phi}\right]d\phi \qquad n>0$$

$$= \frac{1}{2\pi}\int_0^{2\pi} \frac{e^{-jkbR(\phi)}}{R(\phi)}\, e^{j(n+\frac{1}{2})\phi}\; 2j\sin\phi/2\; d\phi$$

The "thin-wire" approximation is that $k^2a^2 << 1$, $a^2 << b^2$. Neglecting terms of this order of magnitude yields

$$A_n = \frac{1}{2\pi}\int_0^{2\pi} \frac{e^{-2jkb\sin\phi/2}}{2\sin\phi/2}\, e^{j(n+\frac{1}{2})\phi}\; 2j\sin\phi/2\; d\phi$$
$$+ \text{ term of order } (a^2/b^2)$$

$$= \frac{j}{\pi}\int_0^{\pi} e^{-2jkb\sin\theta + j(2n+1)\theta}d\theta$$

$$= j\left\{J_{2n+1}(2kb) - j\Omega_{2n+1}(2kb)\right\}$$

where

$$J_{2n+1}(x) = \frac{1}{\pi}\int_0^{\pi} \sin(x\sin\theta - (2n+1)\theta)d\theta$$

is the Bessel function of order 2n+1, and

$$\Omega_{2n+1}(x) = \frac{1}{\pi}\int_0^{\pi} \cos(x\sin\theta - (2n+1)\theta)d\theta$$

is the Lommel-Weber function of order 2n+1, tabulated in Janke-Emde.

Thus, the above result provides a reversion formula for K_n, i.e.,

$$A_n = K_{n+1} - K_n = \Omega_{2n+1}(2kb) + j\,J_{2n+1}(2kb), \qquad n>0$$

Therefore, all that remains to evaluate is K_o. This coefficient can be written as

$$K_o = \frac{1}{2\pi}\int_0^{2\pi} \frac{e^{-jkbR(\phi)}}{R(\phi)}\, d\phi$$

$$= \frac{1}{2\pi}\int_0^{2\pi} \frac{e^{-jkbR(\phi)} - 1}{R(\phi)}\, d\phi + \frac{1}{2\pi}\int_0^{2\pi} \frac{d\phi}{R(\phi)}$$

Now,

$$\frac{1}{2\pi}\int_0^{2\pi} \frac{e^{-jkbR(\phi)} - 1}{R(\phi)}\, d\phi = \frac{1}{2\pi}\int_0^{2\pi} \frac{e^{-2jkb\sin\phi/2} - 1}{2\sin\phi/2}\, d\phi + \text{term } o(a^2/b^2)$$

$$= \int_0^{2kb} dx \left\{ -\frac{j}{\pi}\int_0^{\pi} e^{-jx\sin\phi}\, d\phi \right\}$$

$$= -1/2\int_0^{2kb} \Omega_o(x)dx - j/2 \int_0^{2kb} J_o(x)dx$$

It also can be shown[2]

$$\frac{1}{2\pi}\int_0^{2\pi} \frac{d\phi}{R(\phi)} = \frac{1}{\pi}\ln\frac{8b}{a} + \text{terms } o(a^2/b^2)$$

So, to the order of approximation consistent with original integral equation,

$$K_o = \frac{1}{\pi}\ln\frac{8b}{a} - 1/2\int_0^{2kb} \Omega_o(x)dx - j/2\int_0^{2kb} J_o(x)dx$$

$$A_n = K_{n+1} - K_n = \Omega_{2n+1}(2kb) + j\, J_{2n+1}(2kb)$$

Another expression, useful for determining K_n for large n, can also be found. From the above it is seen that

$$K_n = K_o + \sum_{o}^{n-1} A_n$$

Inserting the integral expressions for A_n yields

$$K_n = K_o + \frac{j}{\pi}\sum_{o}^{n-1}\int_o^{\pi} e^{-2jkb\sin\phi + j(2n+1)\phi}\, d\phi$$

$$= K_o + \frac{j}{\pi}\int_o^{\pi} e^{-2jkb\sin\phi}\left\{\frac{e^{2jn\phi}-1}{\sin\phi}\right\} d\phi$$

Inserting the value for K_o,

$$K_n = \frac{1}{\pi}\ln\frac{8b}{a} + \frac{1}{2\pi}\int_o^{\pi}[e^{-2jkb\sin\phi + 2jn\phi} - 1]\frac{d\phi}{\sin\phi}$$

$$= \frac{1}{\pi}\ln\frac{8b}{a} + \frac{1}{2\pi}\int_o^{\pi}[e^{-2jkb\sin\phi} - 1]\frac{e^{2jn\phi}}{\sin\phi}\, d\phi$$

$$+\frac{1}{2\pi}\int_o^{\pi}[e^{2jn\phi} - 1]\frac{d\phi}{\sin\phi}$$

$$= \frac{1}{\pi}\ln\frac{8b}{a} - \frac{1}{2}\int_o^{2kb}[\Omega_{2n}(x) + j\, J_{2n}(x)]\,dx - \frac{2}{\pi}\sum_{o}^{n-1}\frac{1}{2K+1}$$

This result can be used conveniently to determine the form of K_n for large N. For $n \gg kb$, the integral is small, vanishing in the limit. Thus

$$n \gg 1;\ n > kb,\ K_n \sim \left(\frac{1}{\pi}\ln\frac{8b}{a} - \frac{2}{\pi}\sum_{o}^{n-1}\frac{1}{2K+1}\right) - \frac{j}{2}\int_o^{2kb} J_{2n}(x)\,dx$$

Now, using Sterling's formula to evaluate the harmonic series, it can be shown that

$$\sum_{o}^{n-1}\frac{1}{2K+1} = \frac{\gamma}{2} + \frac{1}{2}\ln 4n,\ \gamma(=.5772) \text{ is Euler's constant.}$$

Similarly, for $n > kb$

$$J_n(x) \cong \frac{1}{\Gamma(n+1)} \left(\frac{x}{2}\right)^n$$

So $K_n \sim \frac{1}{\pi} (\ln \frac{2b}{a} - \gamma - \ln n) - j \frac{(kb)^{n+1}}{\Gamma(2n+2)}$ $\quad \begin{cases} n^2 \gg 1 \\ n > kb \end{cases}$

The Fourier coefficient, a_n, (4), can be written as

$$a_n = (kb - \frac{n^2}{kb}) K_n + kb \left[\frac{A_n - A_{n-1}}{2} \right] .$$

Since A_n vanishes for large n, the asymtotic value of a_n is given by

$$a_n \sim (kb - \frac{n^2}{kb}) \left[\frac{1}{\pi} (\ln \frac{2b}{a} - \gamma - \ln n) - j \frac{(kb)^{2n+1}}{\Gamma(2n+2)} \right] \qquad \begin{cases} n^2 \gg 1 \\ n > kb \end{cases}$$

Finally, (by simple insertion of numerical values), it can be shown that for $k \leqq 2.5$, and $n \geqq 5$, that the asymtotic value of a_n as given above differs negligibly from the correct value.

Appendix B

Input Impedance of Loop Antennas

In the following tables impedances, $Z = R + jX$, are given in ohms and admittances, $Y = 1/Z = G + jB$, are given in mhos. The loop radius is designated by b and the loop wire radius by a. The ratio b/a is expressed in terms of the parameter $\Omega = \ln \frac{2\pi b}{a}$. Note that $2\pi b = c$, the circumference of the loop, and $kb = \frac{2\pi b}{\lambda} = \frac{c}{\lambda}$, where λ is the wavelength. Thus kb is simply the circumference of the loop divided by the wavelength.

Part I: Graphs of the Input Impedance as a function of frequency

Figure B1: R vs. kb for $\Omega = 8, 9, 10, 11, 12$; $kb \leq 2.5$

Figure B2: X vs. kb for $\Omega = 8, 9, 10, 11, 12$; $kb \leq 2.5$

Figure B3: G vs. kb for $\Omega = 8, 9, 10, 11, 12$; $kb \leq 2.5$

Figure B4: B vs. kb for $\Omega = 8, 9, 10, 11, 12$; $kb \leq 2.5$

Figure B5: Locus of Resonance and Anti-Resonance Points

Part II: Tables of Input Impedance and Admittance as a function of frequency.

Table B1: Z and Y vs. kb for $\Omega = 8, 9$; $kb \leq 2.5$

Table B2: Z and Y vs. kb for $\Omega = 10, 11$; $kb \leq 2.5$

Table B3: Z and Y vs. kb for $\Omega = 12$; $kb \leq 2.5$

Part III: Tables of Input Impedance for ka constant

Table B4: Z vs. kb for a = 3/16 in., 1/4 in., 5/16 in. at $\lambda = 100$ cm.

Table B5: Z vs. kb for a = 3/8 in., 1/2 in., 3/4 in., at $\lambda = 100$ cm.

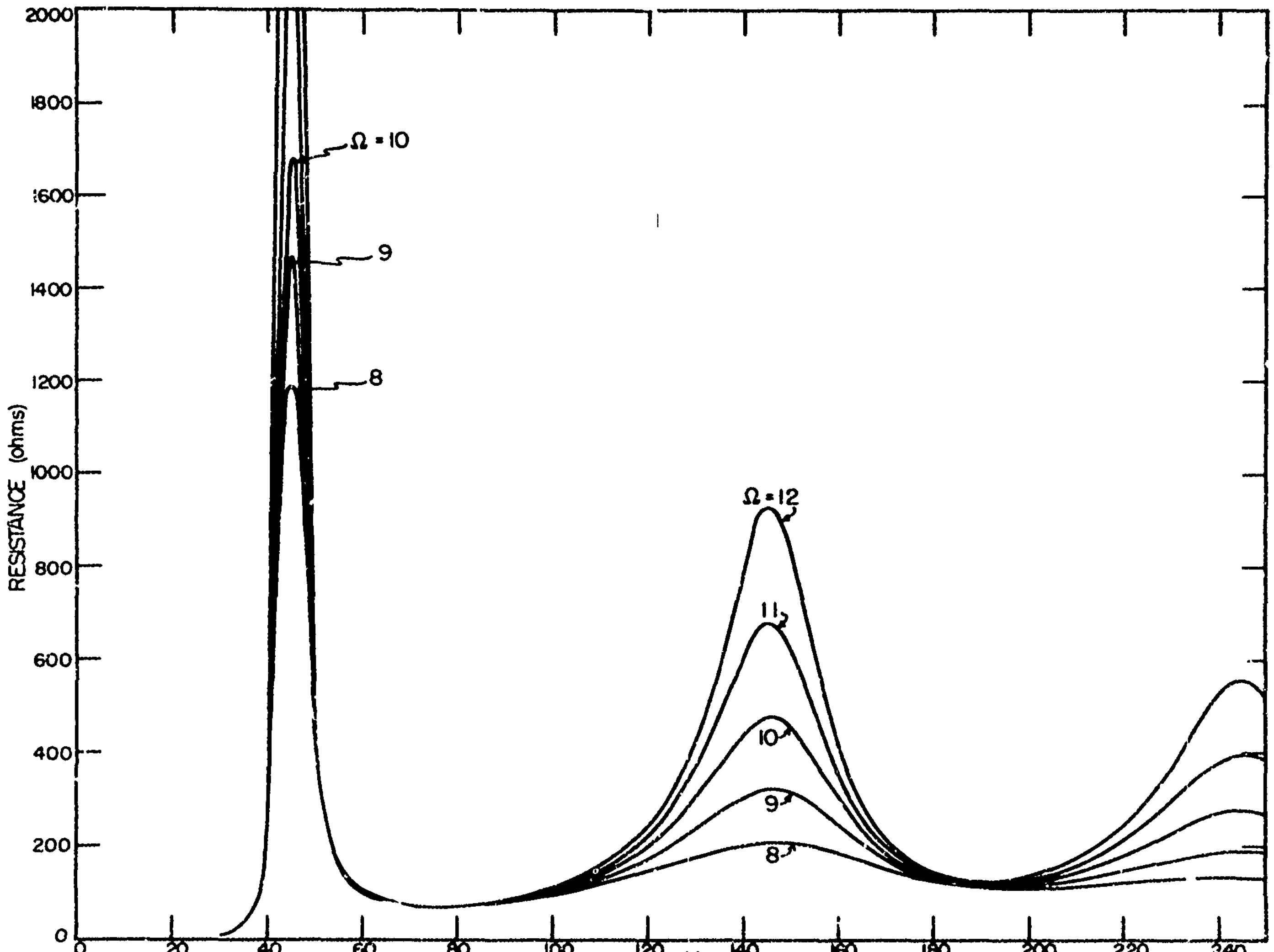

FIG. B1 RESISTANCE OF A LOOP ANTENNA AS A FUNCTION OF FREQUENCY $\Omega = 2\ln(2\pi b/a)$

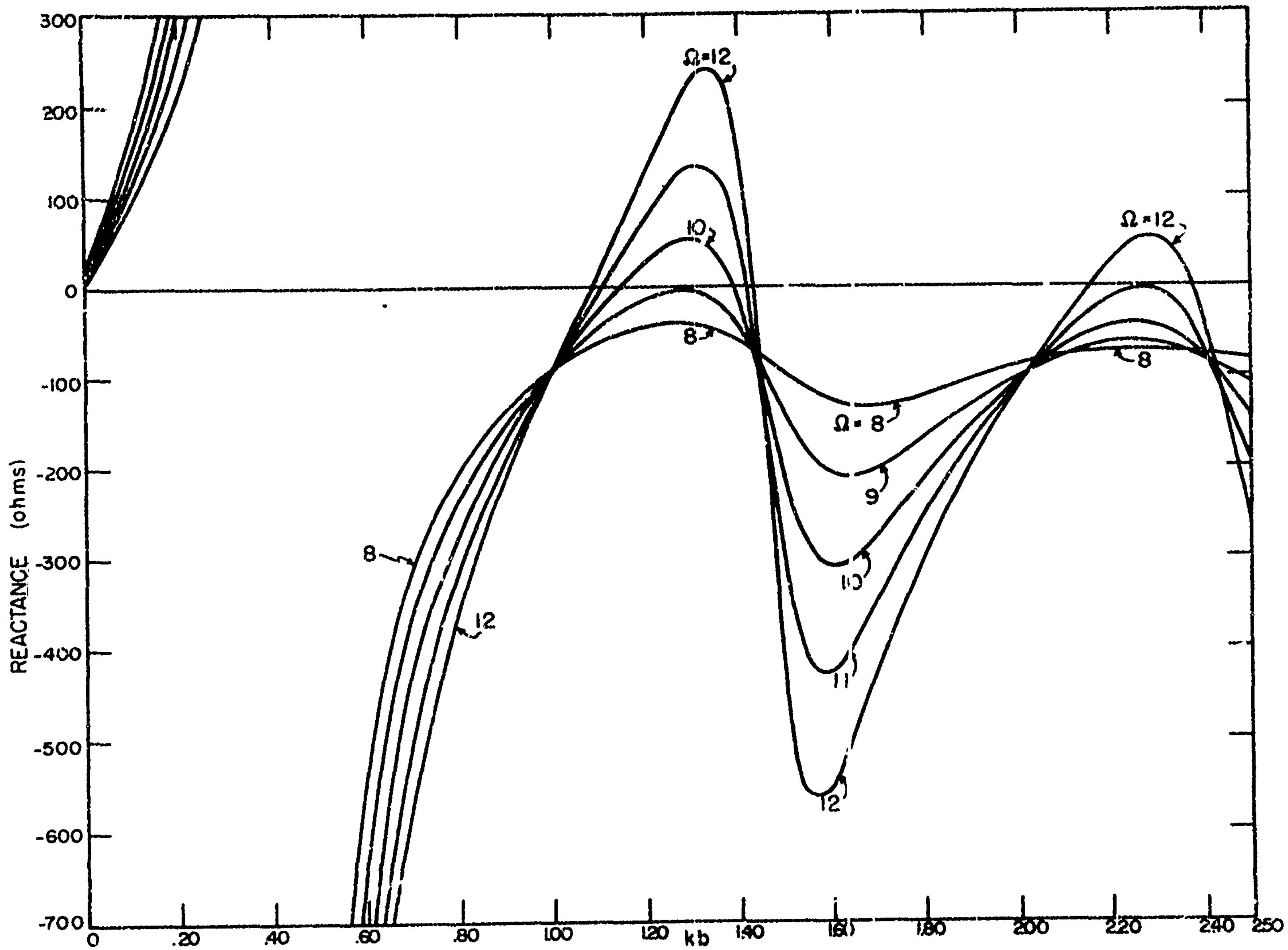

FIG. B2 REACTANCE OF A LOOP ANTENNA AS A FUNCTION OF FREQUENCY $\Omega = 2 \ln(2\pi b/a)$

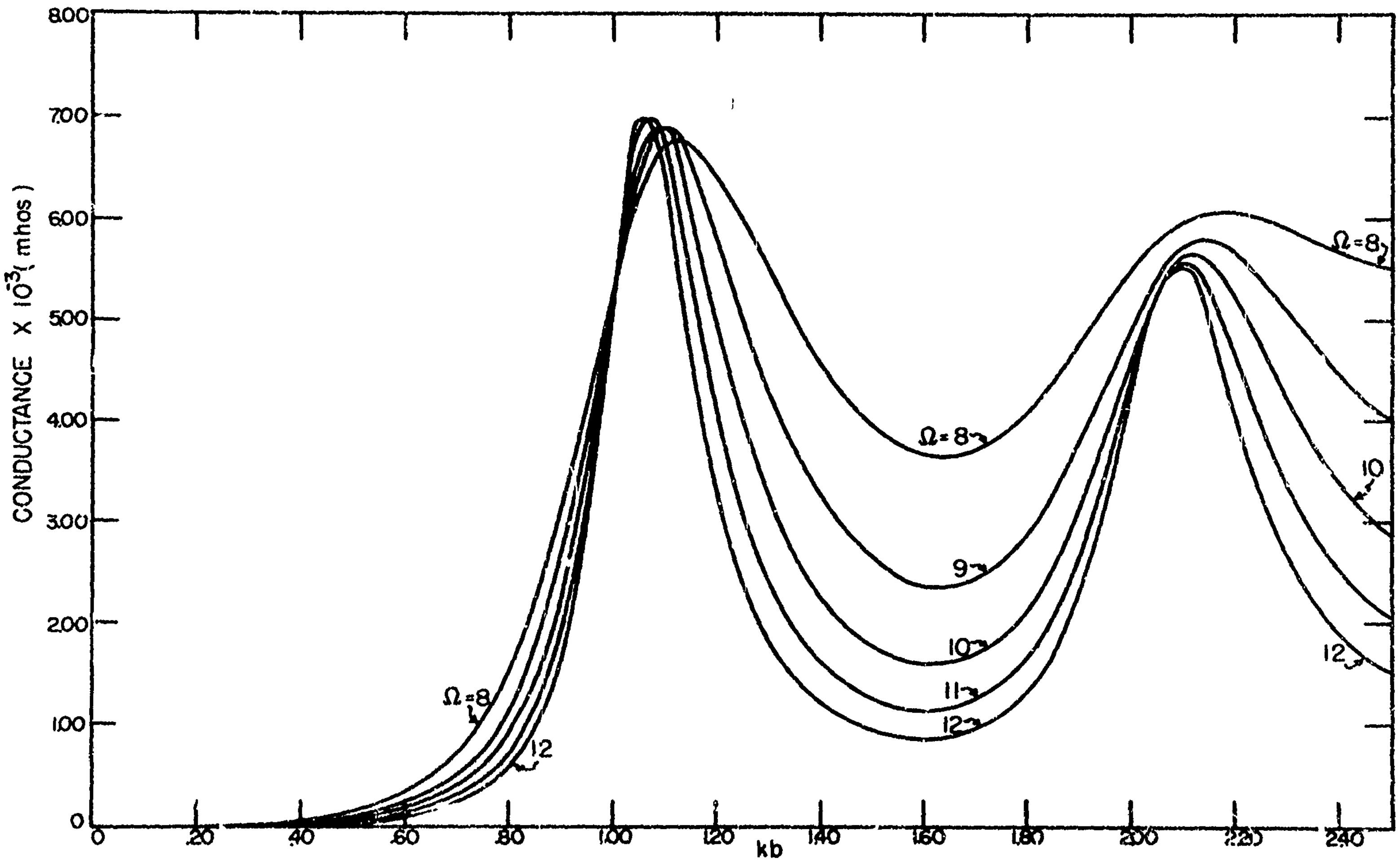

FIG. B3 CONDUCTANCE OF A LOOP ANTENNA AS A FUNCTION OF FREQUENCY $\Omega = 2\ln(2\pi b/a)$

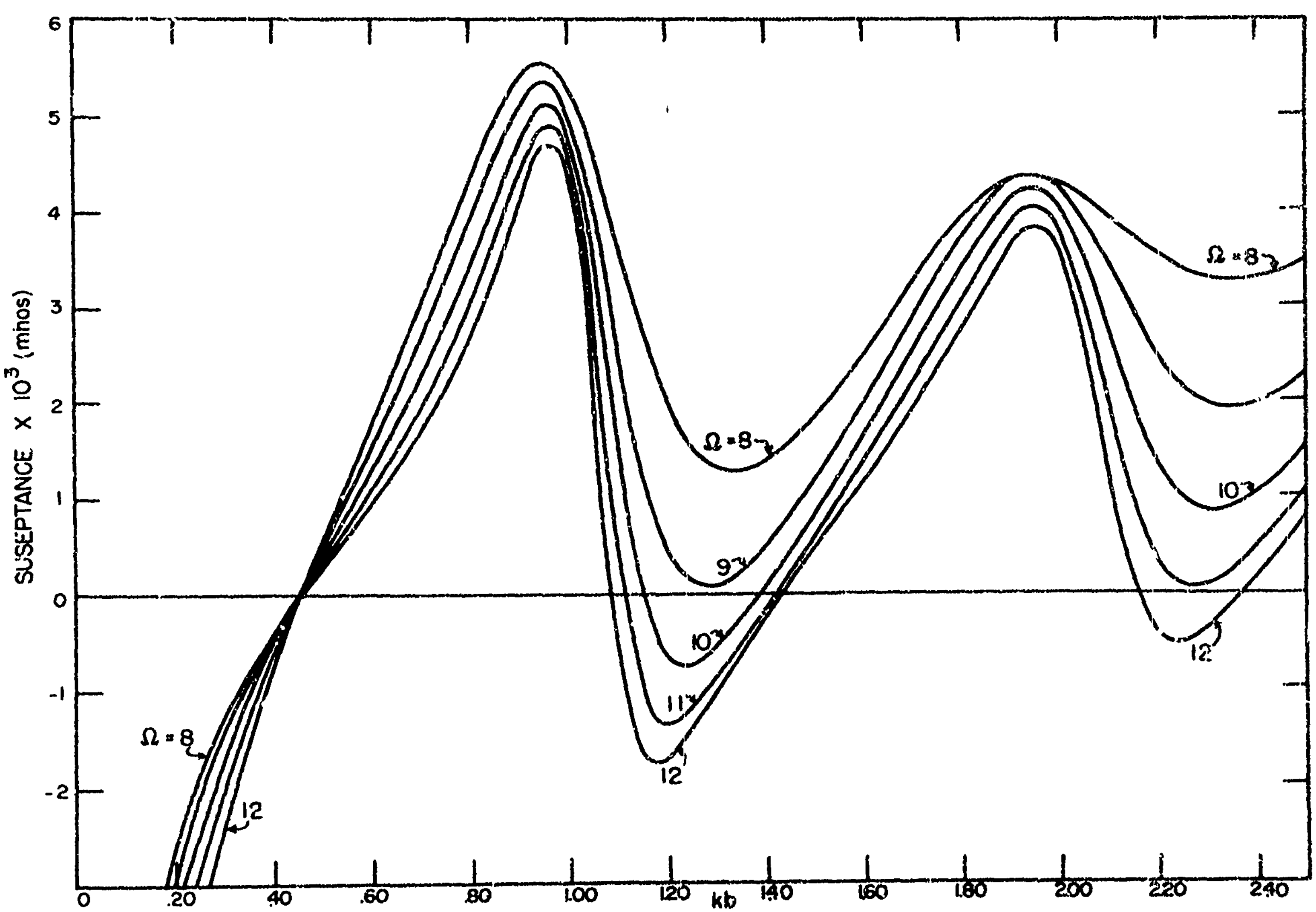

FIG. B4 SUSEPTANCE OF A LOOP ANTENNA AS A FUNCTION OF FREQUENCY $\Omega = 2\ln(2\pi b/a)$

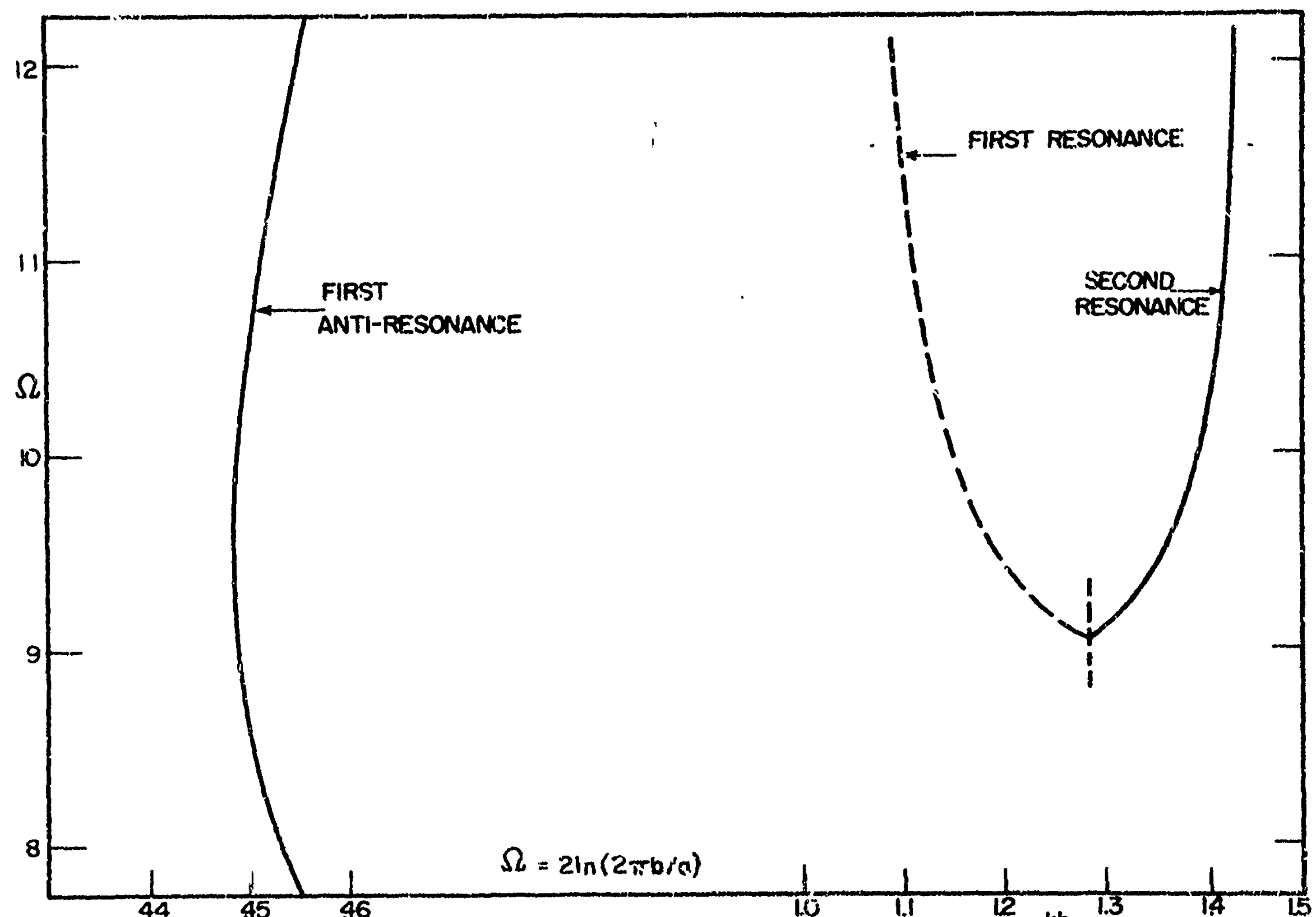

RESONANCE AND ANTI-RESONANCE POINTS FOR LOOP ANTENNA

FIG. B5

TABLE B1

Impedance of Loop Antennae

as a Function of Frequency

$\Omega = 8$, $2\pi b/a = 54.60$ | $\Omega = 9$, $2\pi b/a = 90.02$

R	X	$G \cdot 10^3$	$B \cdot 10^3$	kb	R	X	$G \cdot 10^3$	$B \cdot 10^3$
.0048	43.57	.0025	-22.95	.05	.0046	51.99	.0017	-19.23
.0402	88.77	.0052	-11.36	.10	.0392	107.4	.0034	- 9.311
.[illegible]533	140.5	.0078	- 7.119	.15	.1538	172.0	.0052	- 5.814
.5939	205.7	.0140	- 4.860	.20	.5917	252.2	.0093	- 3.964
1.742	293.1	.0203	- 3.412	.25	1.756	360.6	.0135	- 2.773
6.143	427.4	.0336	- 2.339	.30	6.327	529.1	.0226	- 1.890
23.72	675.2	.0520	- 1.479	.35	25.57	853.2	.0351	- 1.171
140.1	1344.0	.0767	- .7361	.40	162.5	1776.0	.0518	- .5662
7972.7	2189.8	.1172	- .0322	.45	1188.0	-3119.4	.0796	.0209
502.2	-1677.8	.1638	.5471	.50	415.0	-1887.9	.1111	.5054
169.0	- 824.4	.2387	1.164	.55	154.3	- 962.0	.1625	1.013
106.6	- 544.1	.3469	1.770	.60	99.68	- 639.4	.2380	1.527
84.56	- 400.2	.5054	2.392	.65	80.23	- 471.9	.3502	2.060
73.74	- 311.8	.7357	3.028	.70	72.58	- 367.1	.5183	2.622
72.87	- 250.3	1.072	3.683	.75	70.48	- 293.3	.7744	3.223
73.28	- 204.4	1.554	4.335	.80	71.62	- 237.5	1.164	3.860
76.02	- 168.4	2.227	4.934	.85	75.22	- 192.8	1.757	4.502
80.72	- 141.4	3.117	5.376	.90	81.00	- 155.6	2.633	5.057
87.59	- 115.5	4.193	5.531	.95	89.08	- 122.7	3.874	5.337
94.81	- 94.30	5.302	5.274	1.00	98.94	- 95.22	5.247	5.050
104.4	- 77.20	6.193	4.579	1.05	111.8	- 70.25	6.413	4.030
115.4	- 63.08	6.672	3.648	1.10	127.6	- 48.16	6.860	2.589
128.0	- 52.23	6.696	2.732	1.15	147.1	- 29.22	6.541	1.300
142.0	- 44.54	6.412	2.011	1.20	171.2	- 14.36	5.800	.4866
157.4	- 41.09	5.949	1.553	1.25	200.4	- 5.427	4.986	.1350
172.9	- 41.89	5.462	1.323	1.30	234.0	- 4.986	4.271	.0910
188.1	- 48.12	4.991	1.277	1.35	270.2	- 17.55	3.686	.2394
200.7	- 60.73	4.565	1.382	1.40	302.2	- 46.51	3.232	.4975
207.4	- 76.86	4.240	1.571	1.45	320.5	- 91.53	2.885	.8239
207.5	- 95.54	3.977	1.831	1.50	315.5	- 142.0	2.636	1.186
199.8	- 113.3	3.788	2.148	1.55	287.5	- 184.7	2.462	1.581
186.0	- 126.1	3.684	2.497	1.60	247.0	- 207.6	2.373	1.994
169.5	- 132.7	3.657	2.864	1.65	206.3	- 211.7	2.361	2.423
152.8	- 133.1	3.722	3.242	1.70	172.5	- 202.6	2.437	2.862
138.7	- 128.9	3.869	3.595	1.75	147.8	- 186.7	2.607	3.293

TABLE B1
(Continued)

R	X	$G \cdot 10^3$	$B \cdot 10^3$	kb	R	X	$G \cdot 10^3$	$B \cdot 10^3$
127.8	-121.6	4.106	3.909	1.80	130.9	-168.1	2.883	3.703
119.5	-112.6	4.415	4.158	1.85	121.7	-149.6	3.273	4.023
115.4	-104.2	4.775	4.310	1.90	114.6	-131.4	3.774	4.282
113.2	- 95.82	5.146	4.356	1.95	114.8	-115.1	4.345	4.357
113.4	- 88.39	5.485	4.275	2.00	117.0	-101.6	4.915	4.226
114.4	- 82.18	5.766	4.142	2.05	121.7	- 87.95	5.398	3.902
116.8	- 77.20	5.958	3.938	2.10	128.8	- 77.59	5.697	3.432
119.9	- 73.74	6.050	3.720	2.15	137.4	- 70.01	5.776	2.941
123.2	- 71.84	6.056	3.531	2.20	148.0	- 64.94	5.665	2.485
126.2	- 71.22	6.001	3.385	2.25	159.1	- 63.49	5.421	2.163
129.3	- 71.99	5.903	3.286	2.30	170.4	- 65.77	5.108	1.972
131.1	- 73.82	5.792	3.263	2.35	180.0	- 72.08	4.788	1.918
131.9	- 76.29	5.681	3.286	2.40	186.8	- 81.78	4.492	1.966
131.7	- 79.05	5.581	3.349	2.45	190.6	- 94.78	4.206	2.091
130.1	- 81.71	5.512	3.461	2.50	187.8	-106.4	4.031	2.284

TABLE B2

Impedance of Loop Antennae

Ω = 10; 2πb/a = 148.41 (left columns) — Ω = 11; 2πb/a = 244.69 (right columns)

R	X	G · 10³	B · 10³	kb	R	X	G · 10³	B · 10³
.0051	62.59	.0013	-15.98	.05	.0047	72.24	.0009	-13.84
.0410	128.0	.0025	- 7.812	.10	.0411	147.0	.0019	- 6.803
.1577	203.7	.0038	- 4.908	.15	.1532	233.9	.0028	- 4.275
.5936	297.7	.0067	- 3.360	.20	.5991	342.7	.0051	- 2.918
1.777	425.8	.0098	- 2.348	.25	1.744	488.8	.0073	- 2.046
6.355	624.4	.0163	- 1.601	.30	6.263	713.6	.0123	- 1.401
25.47	1003.1	.0253	- .9963	.35	24.43	1136.6	.0189	- .8793
159.7	2063.4	.0373	- .4818	.40	149.1	2294.6	.0282	- .4339
1679.4	-3205.9	.0571	.0109	.45	2263.2	5631.6	.0430	- .0107
468.8	-2250.5	.0887	.4258	.50	479.5	-2768.6	.0607	.3505
156.6	-1142.6	.1177	.8590	.55	167.7	-1360.8	.0892	.7238
100.7	- 756.0	.1731	1.300	.60	100.0	- 891.3	.1316	1.106
80.95	- 555.7	.2567	1.762	.65	84.42	- 650.5	.1962	1.512
73.25	- 430.4	.3842	2.258	.70	75.87	- 500.7	.2959	1.952
71.23	- 341.9	.5841	2.803	.75	73.50	- 394.9	.4556	2.448
72.60	- 274.3	.9018	3.407	.80	74.78	- 314.0	.7175	3.013
76.57	- 219.5	1.416	4.061	.85	78.92	- 248.3	1.162	3.657
82.99	- 173.3	2.248	4.694	.90	85.67	- 192.1	1.937	4.342
91.97	- 132.5	3.534	5.093	.95	95.37	- 141.5	3.274	4.859
103.7	- 95.58	5.214	4.808	1.00	108.1	- 95.57	5.192	4.591
119.2	- 61.60	6.621	3.422	1.05	125.5	- 51.61	6.816	2.804
138.9	- 29.61	6.884	1.468	1.10	148.3	- 8.771	6.720	.3974
164.8	- 12.50	6.067	.0046	1.15	179.4	33.22	5.389	- .9979
199.2	25.90	4.936	- .6415	1.20	222.4	73.70	4.051	- 1.342
244.4	45.67	3.954	- .7390	1.25	282.8	109.6	3.074	- 1.192
302.2	53.12	3.210	- .5642	1.30	367.3	132.4	2.410	- .8682
371.0	37.06	2.669	- .2666	1.35	480.3	121.7	1.956	- .4955
438.4	- 16.75	2.278	.0870	1.40	604.5	50.75	1.643	- .1379
475.9	- 109.9	1.995	.4607	1.45	677.1	- 122.7	1.430	.2592
455.1	- 214.2	1.799	.8465	1.50	627.6	- 308.0	1.284	.6302
384.9	- 286.2	1.673	1.244	1.55	491.3	- 412.2	1.195	1.002
302.8	- 309.7	1.614	1.651	1.60	355.3	- 425.4	1.156	1.385
234.4	- 299.8	1.619	2.070	1.65	260.3	- 393.3	1.170	1.768
185.2	- 274.2	1.692	2.504	1.70	198.2	- 346.3	1.245	2.175
153.5	- 242.6	1.863	2.944	1.75	162.4	- 295.3	1.430	2.600

TABLE B2
(Continued)

R	X	$G \cdot 10^3$	$B \cdot 10^3$	kb	R	X	$G \cdot 10^3$	$B \cdot 10^3$
133.7	-211.3	2.139	3.380	1.80	138.1	-253.9	1.653	3.040
122.6	-181.7	2.551	3.731	1.85	126.3	-213.3	2.055	3.471
118.1	-154.5	3.122	4.086	1.90	122.1	-176.4	2.653	3.832
118.5	-129.8	3.836	4.202	1.95	124.0	-142.6	3.471	3.994
123.2	-107.5	4.610	4.019	2.00	130.5	-111.5	4.429	3.786
131.6	- 87.41	5.272	3.500	2.05	142.1	- 82.63	5.259	3.058
143.9	- 69.91	5.625	2.732	2.10	159.2	- 56.28	5.583	1.974
159.8	- 55.64	5.580	1.942	2.15	182.5	- 33.00	5.307	.9598
179.6	- 45.83	5.228	1.335	2.20	212.8	- 15.14	4.678	.3328
202.5	- 41.74	4.737	.9764	2.25	250.7	- 4.160	3.988	.0662
227.6	- 45.36	4.226	.8424	2.30	295.8	- 6.389	3.380	.0730
251.3	- 58.68	3.774	.8812	2.35	342.5	- 27.26	2.901	.2309
269.6	- 81.82	3.397	1.031	2.40	379.2	- 70.53	2.535	.4715
277.5	-112.5	3.094	1.255	2.45	397.6	-132.8	2.263	.7559
271.3	-144.3	2.873	1.528	2.50	381.6	-196.0	2.074	1.065

TABLE B3

Impedance of Loop Antennae

$\Omega = .12$; $2\pi b/a = 403.43$

kb	R	X	$G \cdot 10^3$	$B \cdot 10^3$
.05	.0053	81.46	.0008	-12.28
.10	.0419	167.0	.0015	- 5.986
.15	.1548	265.3	.0022	- 3.769
.20	.5967	386.2	.0040	- 2.589
.25	1.721	549.5	.0057	- 1.820
.30	6.042	797.4	.0095	- 1.254
.35	23.50	1255.6	.0149	- .7962
.40	131.5	2446.6	.0219	- .4076
.45	1465.2	14,782.6	.0337	- .0340
.50	588.8	-3477.0	.0474	.2799
.55	185.6	-1617.7	.0700	.6102
.60	106.1	-1011.2	.1033	.9842
✓.65	89.32	- 754.6	.1547	1.307
.70	79.48	- 576.3	.2348	1.703
.75	76.52	- 451.4	.3650	2.153
.80	77.56	- 356.1	.5839	2.631
.85	81.63	- 276.4	.9698	3.308
.90	88.50	- 211.6	1.682	4.022
.95	98.43	- 151.5	3.017	4.642
1.00	112.0	- 95.32	5.178	4.406
1.05	130.5	- 41.05	6.974	- 2.194
1.10	155.3	13.30	6.393	- .5478
1.15	190.7	67.58	4.660	- 1.652
1.20	239.[illegible]	125.4	3.278	- 1.718
1.25	312.5	181.6	2.392	- 1.390
1.30	422.0	227.9	1.834	- .9905
1.35	584.2	236.5	1.471	- 5954
1.40	788.1	142.3	1.229	- .2218
1.45	926.1	- 116.0	1.063	.1332
1.50	837.1	- 419.6	.9546	.4785
1.55	610.9	- 559.7	.8899	.8153
1.60	414.5	- 554.2	.8654	1.157
1.65	287.7	- 493.0	.8829	1.513
1.70	212.5	- 422.5	.9503	1.889
1.75	168.8	- 356.6	1.085	2.291

TABLE B3
(Continued)

kb	R	X	$G \cdot 10^3$	$B \cdot 10^3$
1.80	144.0	-297.6	1.317	2.722
1.85	131.3	-245.3	1.696	3.168
1.90	123.8	-193.8	2.295	3.594
1.95	129.7	-154.6	3.185	3.796
2.00	137.6	-113.9	4.314	3.571
2.05	151.7	- 75.20	5.292	2.623
2.10	172.7	- 38.28	5.518	1.223
2.15	195.8	- 36.02	4.941	.0909
2.20	243.0	26.49	4.067	- .4433
2.25	257.2	48.43	3.277	- .5340
2.30	367.0	53.74	2.668	- .3907
2.35	447.1	28.71	2.227	- .1430
2.40	520.0	- 39.84	1.912	.1465
2.45	552.7	-148.0	1.688	.4522
2.50	521.0	-259.2	1.538	.7641

TABLE B4

Input Impedance for ka Constant

	a = 3/16 in at λ = 100 cm		a = 1/4 in at λ = 100 cm		a = 5/16 in at λ = 100 cm		
Kb	R	X	R	X	R	X	Kb
.05							.05
.10							.10
.15		149		133			.15
.20		244		217		196	.20
.25	2	385	2	357		313	.25
.30	7	625	6	526	6	500	.30
.35	25	999	27	908	23	801	.35
.40	172	2209	167	1986	169	1871	.40
.45	19992	-3998	15202	-5153	13535	-3981	.45
.50	376	-2320	408	-2251	410	-2094	.50
.55	170	-1348	152	-1200	129	- 963	.55
.60	104	- 905	103	- 820	103	- 767	.60
.65	85	- 670	83	- 613	81	- 570	.65
.70	77	- 525	75	- 486	74	- 455	.70
.75	75	- 422	73	- 391	72	- 367	.75
.80	76	- 342	75	- 317	74	- 298	.80
.85	81	- 270	80	- 255	78	- 242	.85
.90	89	- 210	87	- 197	86	- 188	.90
.95	98	- 155	97	- 150	95	- 142	.95
1.00	112	- 102	110	- 95	108	- 95	1.00
1.05	132	- 39	129	- 45	126	- 50	1.05
1.10	157	20	154	6	151	- 3	1.10
1.15	195 Ω	81	189	60	184	45	1.15
1.20	245 (12.447)	152	238	118	231	95	1.20
1.25			311	178	299	145	1.25
1.30			426	229	402	186	1.30
1.35			589	244	547	191	1.35
1.40			836	167	739	118	1.40
1.45			988	- 108	853	- 119	1.45
1.50			918	- 448	800	- 400	1.50
1.55			689 Ω	- 613	600	- 547	1.55
1.60			447 (12.446)	- 623	418	- 553	1.60
1.65					289	- 497	1.65
1.70					215	- 434	1.70
1.75					170	- 365	1.75
1.80					146	- 309	1.80
1.85					134	- 252	1.85
1.90					126	- 200	1.90
1.95					132	- 160	1.95
2.00					141 Ω	- 113	2.00
2.05					157 (12.494)	- 72	2.05

TABLE B5

Input Impedance of Loop Antenna for ka Constant

	a = 3/8 in at λ = 100 cm		a = 1/2 in at λ = 100 cm		a = 3/4 in at λ = 100 cm		
Kb	R	X	R	X	R	X	Kb
.05							.05
.10							.10
.15							.15
.20							.20
.25	2	278					.25
.30	6	454	6	416			.30
.35	24	768	22	666			.35
.40	171	1738	146	1456			.40
.45	1216	-3160	1052		6772	2646	.45
.50	400	-1959	431	-1821	513	-1660	.50
.55	153	-1053	157	- 954	166	- 837	.55
.60	100	- 716	95	- 653	103	- 570	.60
.65	81	- 542	80	- 495	82	- 435	.65
.70	73	- 430	73	- 390	73	- 345	.70
.75	72	- 348	71	- 318	71	- 280	.75
.80	73	- 283	72	- 261	72	- 232	.80
.85	78	- 230	76	- 215	76	- 192	.85
.90	84	- 182	83	- 170	82	- 158	.90
.95	94	- 138	92	- 133	90	- 125	.95
1.00	106	- 95	104	- 95	101	- 95	1.00
1.05	124	- 53	122	- 60	115	- 67	1.05
1.10	148	- 12	142	- 23	134	- 40	1.10
1.15	179	33	171	13	158	- 11	1.15
1.20	224	77	212	48	192	13	1.20
1.25	287	120	268	83	234	33	1.25
1.30	379	150	343	98	291	41	1.30
1.35	511	151	448	94	361	30	1.35
1.40	661	80	560	35	434	- 15	1.40
1.45	774	- 123	632	- 116	487	- 112	1.45
1.50	719	- 353	617	- 295	476	- 264	1.50
1.55	552	- 497	492	- 410	402	- 307	1.55
1.60	389	- 508	356	- 428	316	- 337	1.60
1.65	280	- 460	254	- 404	243	- 327	1.65
1.70	210	- 405	202	- 360	191	- 300	1.70
1.75	168	- 343	164	- 310	159	- 265	1.75

TABLE B5

(Continued)

	a = 3/8 in at λ = 100 cm		a = 1/2 in at λ = 100 cm		a = 3/4 in at λ = 100 cm		
Kb	R	X	R	X	R	X	Kb
1.80	143	-291	140	-266	136	-232	1.80
1.85	133	-241	128	-225	125	-200	1.85
1.90	124	-193	122	-182	118	-168	1.90
1.95	130	-155	126	-150	122	-138	1.95
2.00	138	-112	134	-111	128	-110	2.00
2.05	153	- 75	147	- 79	139	- 85	2.05
2.10	181	- 35	170	- 45	156	- 60	2.10
2.15	211	5	193	- 15	179	- 40	2.15
2.20	250	40	235	15	209	- 18	2.20
2.25	310	65	286	34	248	- 5	2.25
2.30	395	80	353	39	294	- 8	2.30
2.35	489	53	427	16	343	- 27	2.35
2.40	598	- 25	499	- 42	387	- 70	2.40
2.45	653 Ω (12.486)	-174	541	-148	409	-136	2.45
2.50			517 Ω (11.951)	-262	398 Ω (11.141)	-201	2.50

Appendix C

Graphs to Facilitate Evaluation of the Current Distribution on a Loop Antenna

The current distribution on a loop antenna is given explicitly by equation (20)

$$I(\phi) = \frac{V}{j\pi\zeta_o}\left\{\frac{1}{a_o} + 2\sum_{1}^{4}\frac{\cos n\phi}{a_n} - \frac{2\pi}{\ln\frac{n_o}{4.5}}\left[\left(\frac{kb}{4.5}\right)J_1(\phi) + \left(\frac{kb}{4.5}\right)^3 J_2(\phi)\right]\right\} \qquad kb \leqq 2.5$$

where

V is the voltage driving the antenna

ζ_o = 120 ohms

a = radius of antenna wire

b = radius of antenna

$k = \omega/c = 2\pi/\lambda$

$\ln(n_o/4.5) = \frac{\Omega}{2} - 3.226$

$\Omega = 2\ln\frac{2\pi b}{a}$

To facilitate evaluation of this formula, the succeeding pages contain the following graphs:

Figure C1: $\mathrm{Re}(1/a_o)$; Ω = 8, 9, 10, 11, 12, $kb \leqq 2.5$

Figure C2: $\mathrm{Im}(1/a_o)$; Ω = 8, 9, 10, 11, 12, $kb \leqq 2.5$

Figure C3: $\mathrm{Re}(1/a_1)$; Ω = 8, 9, 10, 11, 12, $kb \leqq 2.5$

Figure C4: $\mathrm{Im}(1/a_1)$; Ω = 8, 9, 10, 11, 12, $kb \leqq 2.5$

Figure C5: $\mathrm{Re}(1/a_2)$; Ω = 8, 9, 10, 11, 12, $kb \leqq 2.5$

Figure C6: $\mathrm{Im}(1/a_2)$; Ω = 8, 9, 10, 11, 12, $kb \leqq 2.5$

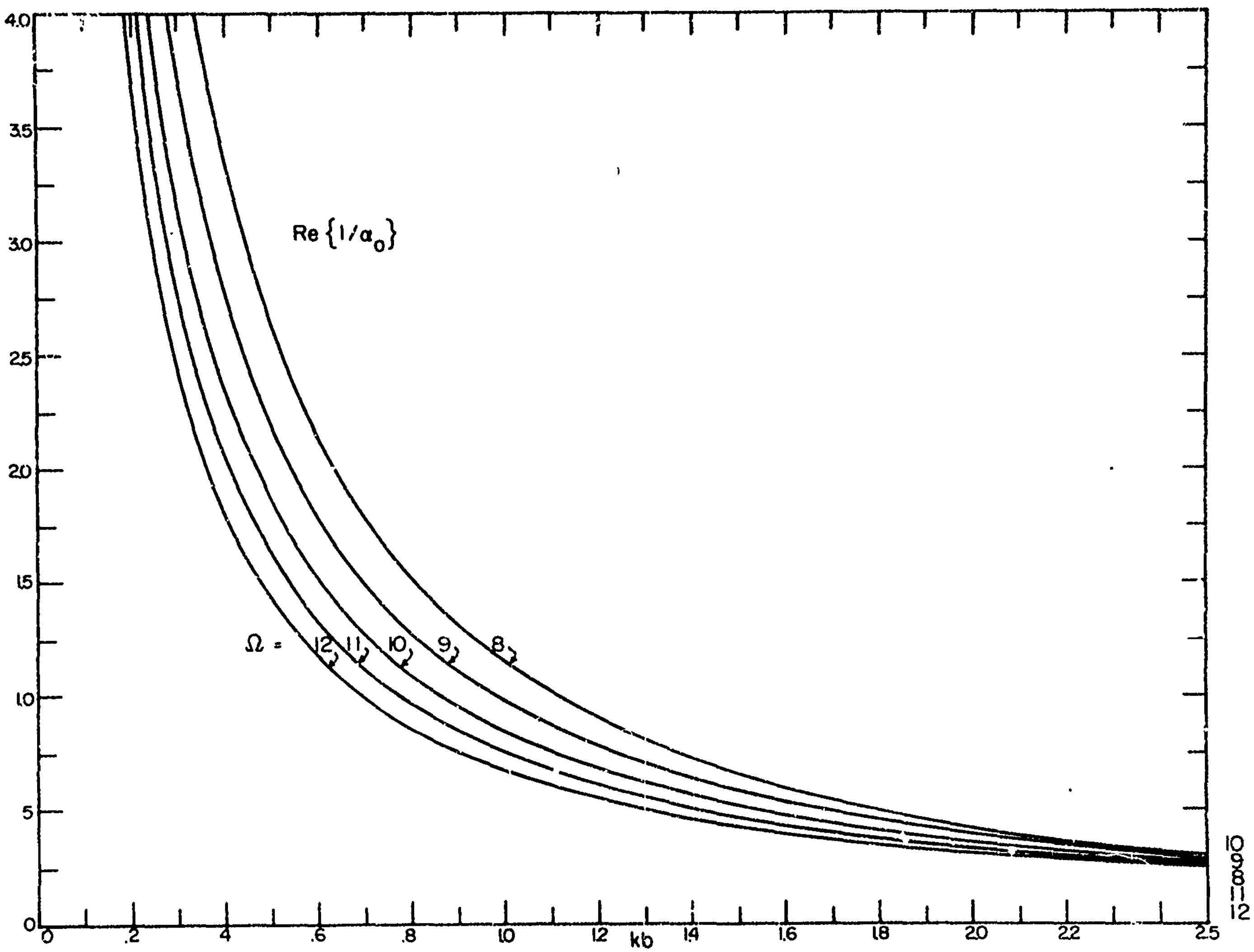

Re {1/α₀}
Ω = 12 11 10 9 8
10
9
8
11
12
4.0
3.5
3.0
2.5
2.0
1.5
1.0
5
0
0
.2
.4
.6
.8
1.0
1.2
1.4
1.6
1.8
2.0
2.2
2.5
kb

FIG. c1

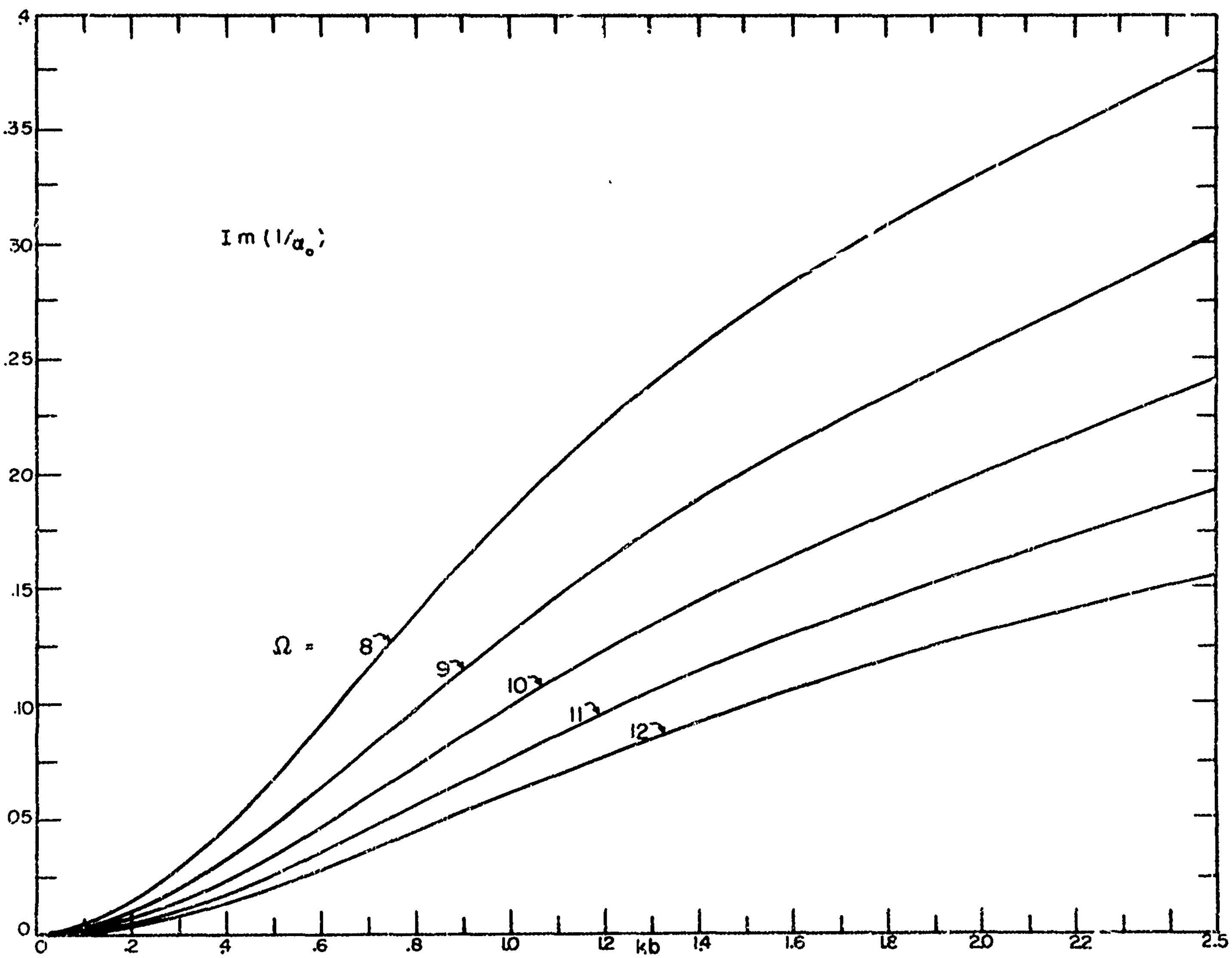
Im (1/a₀)
Ω = 8
9
10
11
12
kb
0
.05
.10
.15
.20
.25
.30
.35
.4
.2
.4
.6
.8
1.0
1.2
1.4
1.6
1.8
2.0
2.2
2.5

FIG. c 2

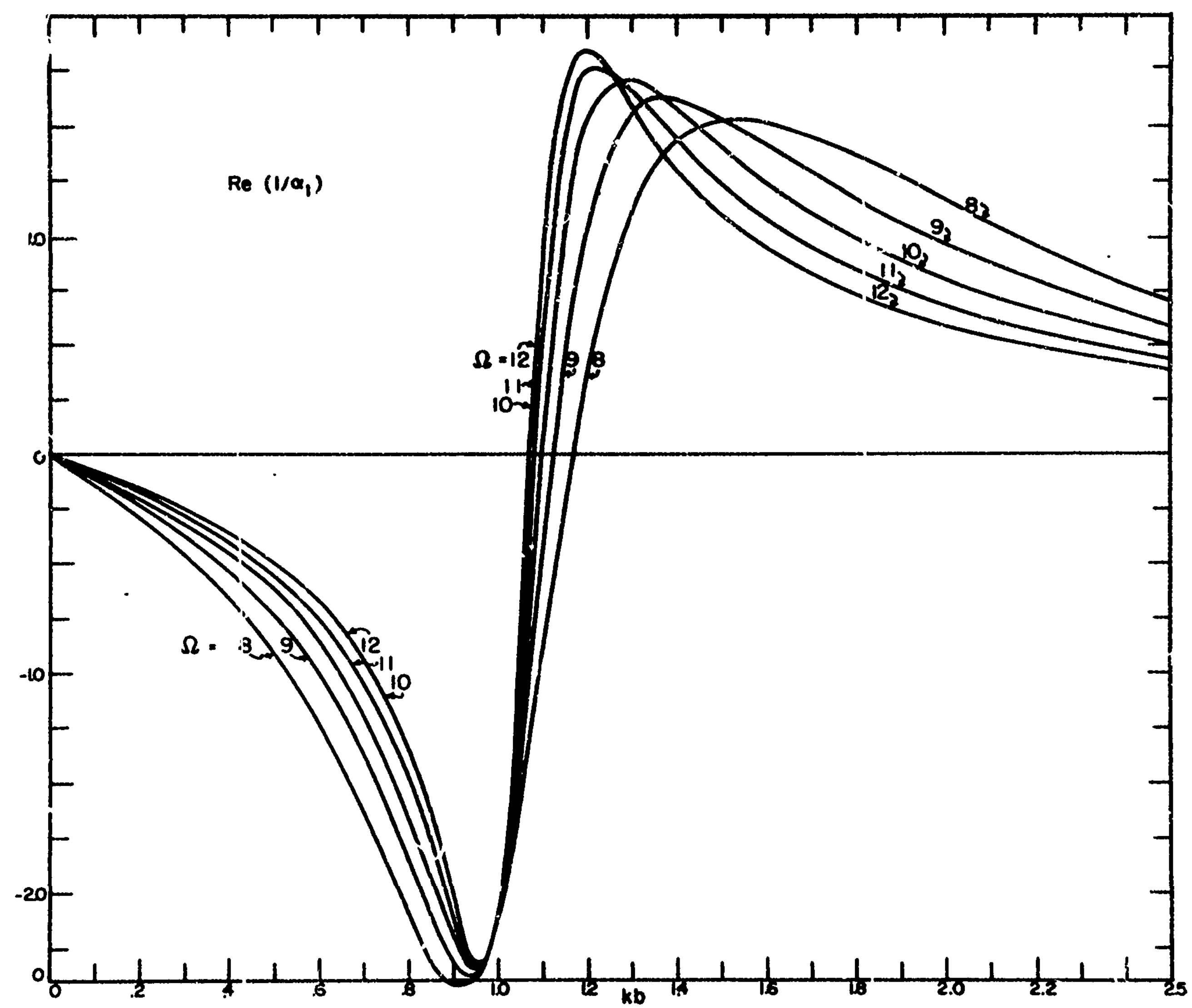
Re (1/α1)
Ω = 12
11
10
9
8
Ω = .8
.9
12
11
10
.8
.9
10
11
12
0
.2
.4
.6
.8
1.0
1.2
1.4
1.6
1.8
2.0
2.2
2.5
kb
5.0
0
-10
-20

FIG. c3

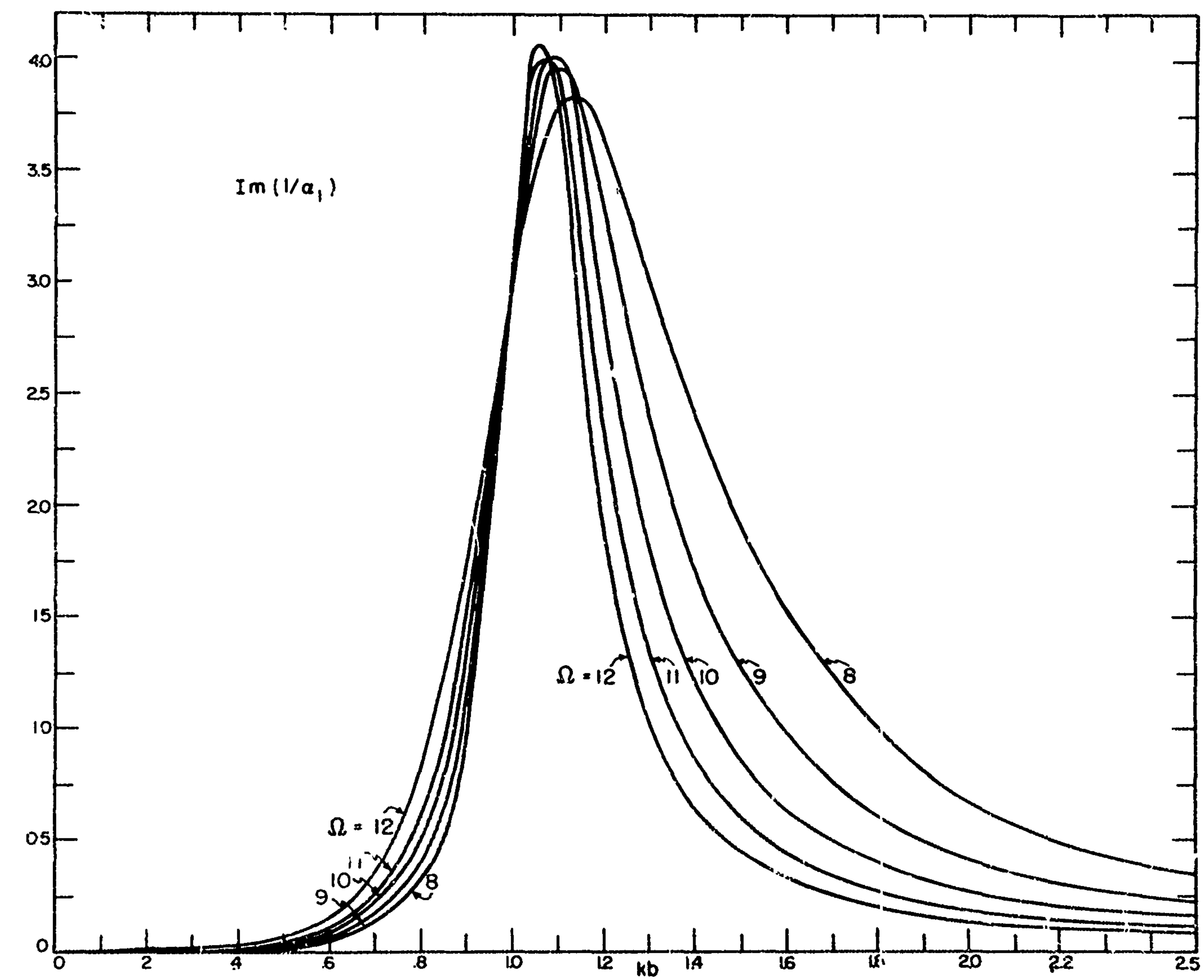
Im(1/a1)
Ω = 12
11
10
9
8
kb
0
2
4
.6
.8
1.0
1.2
1.4
1.6
2.0
2.2
2.5
0.5
1.0
1.5
2.0
2.5
3.0
3.5
4.0
FIG. c4

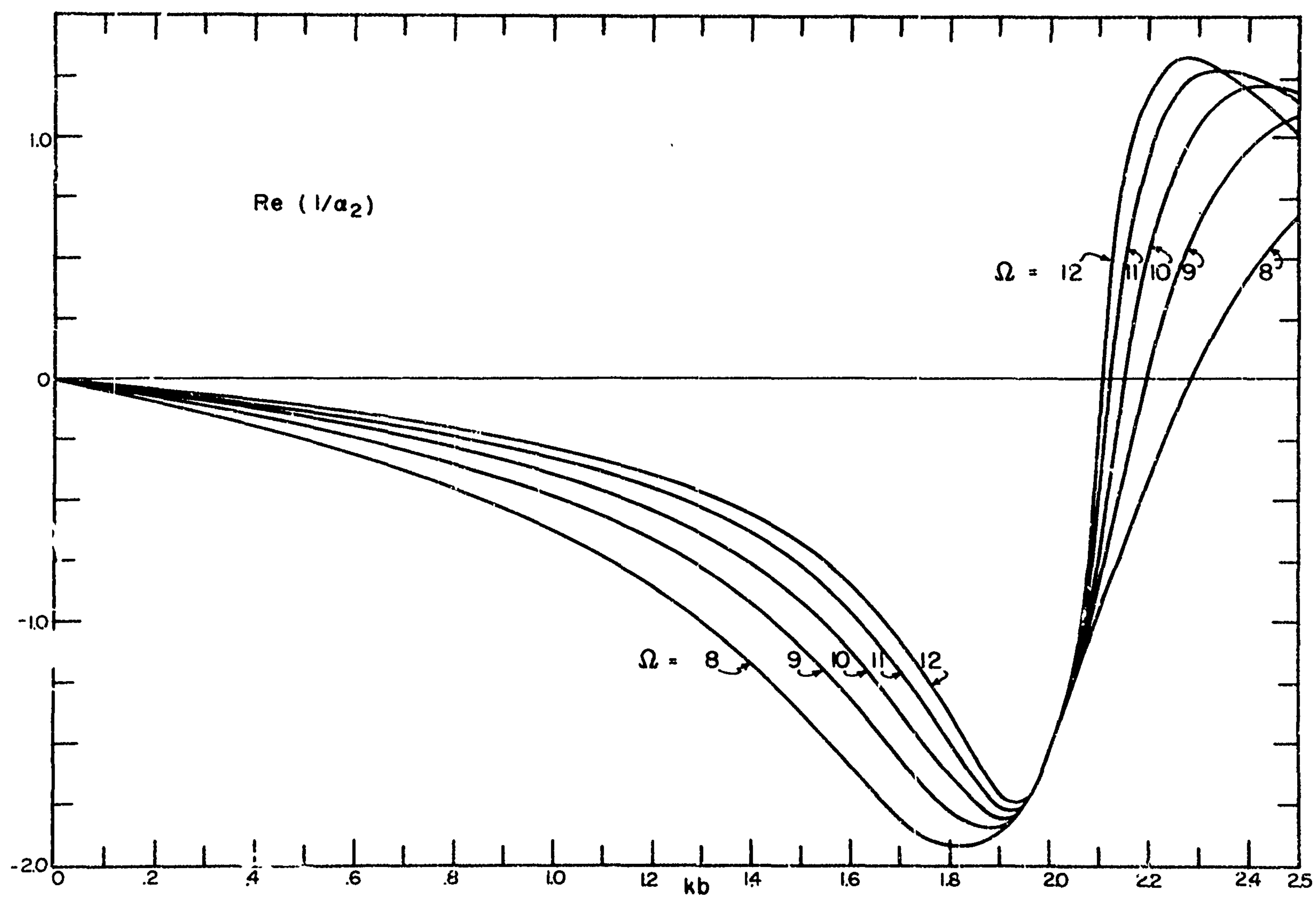
Re (1/a2)
1.0
0
-1.0
-2.0
0
.2
.4
.6
.8
1.0
1.2
1.4
1.6
1.8
2.0
2.2
2.4
2.5
kb
Ω = 12
11
10
9
8
Ω = 8
9
10
11
12

FIG. c5

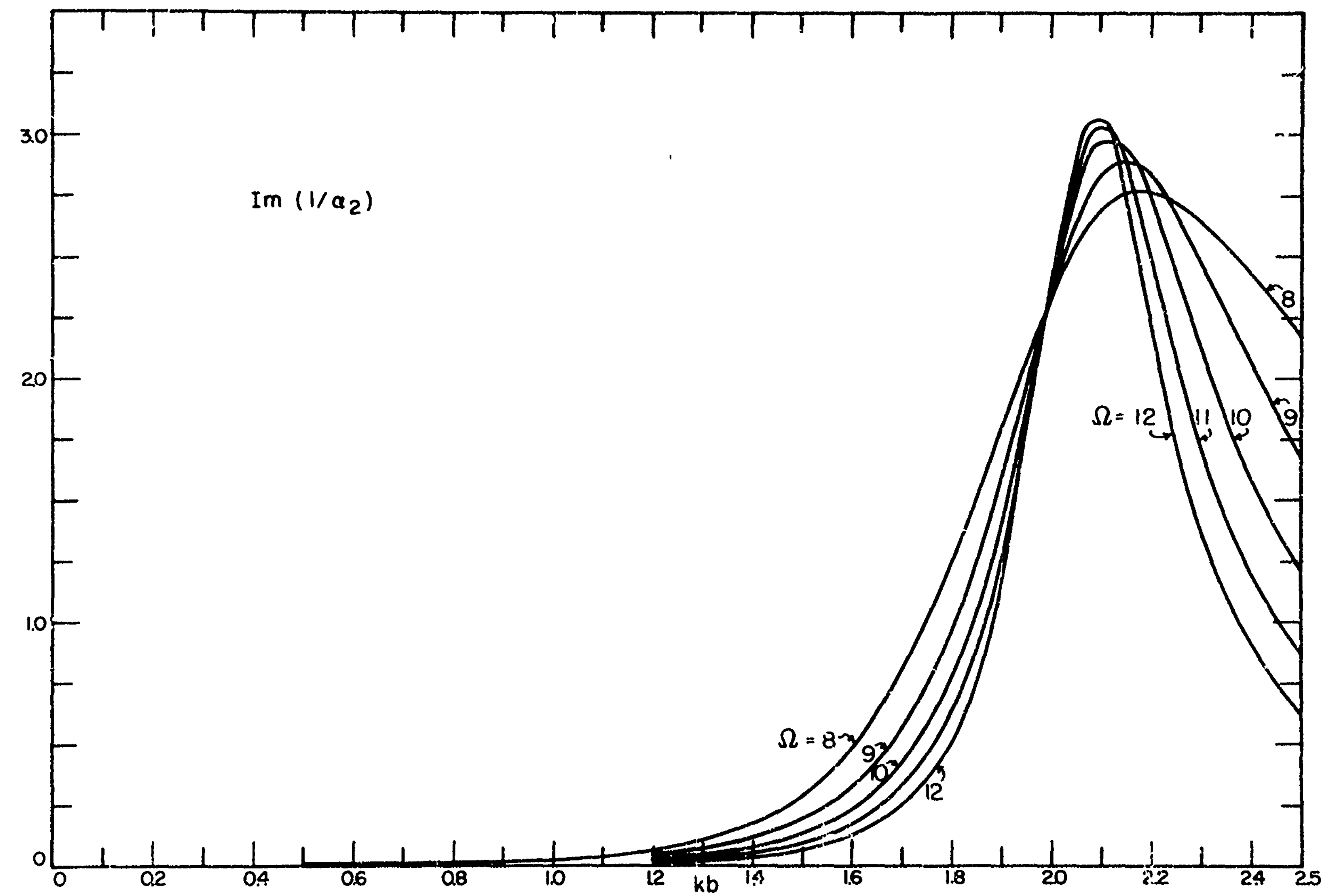

Im (1/a2)
3.0
2.0
1.0
0
0.2
0.4
0.6
0.8
1.0
1.2
1.4
1.6
1.8
2.0
2.2
2.4
2.5
kb
Ω = 8
9
10
12
Ω = 12
11
10
9
8

FIG. c6

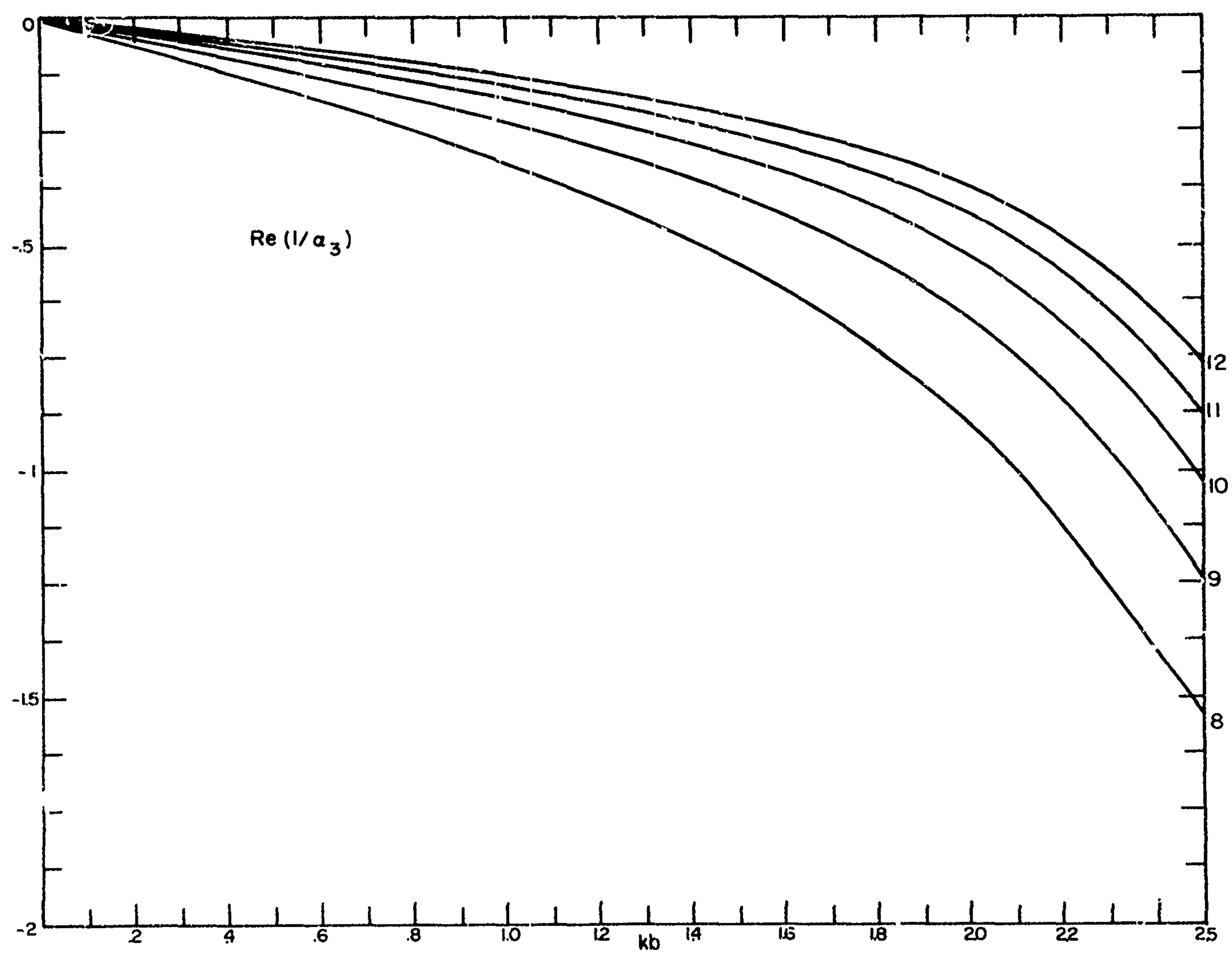

FIG. c7

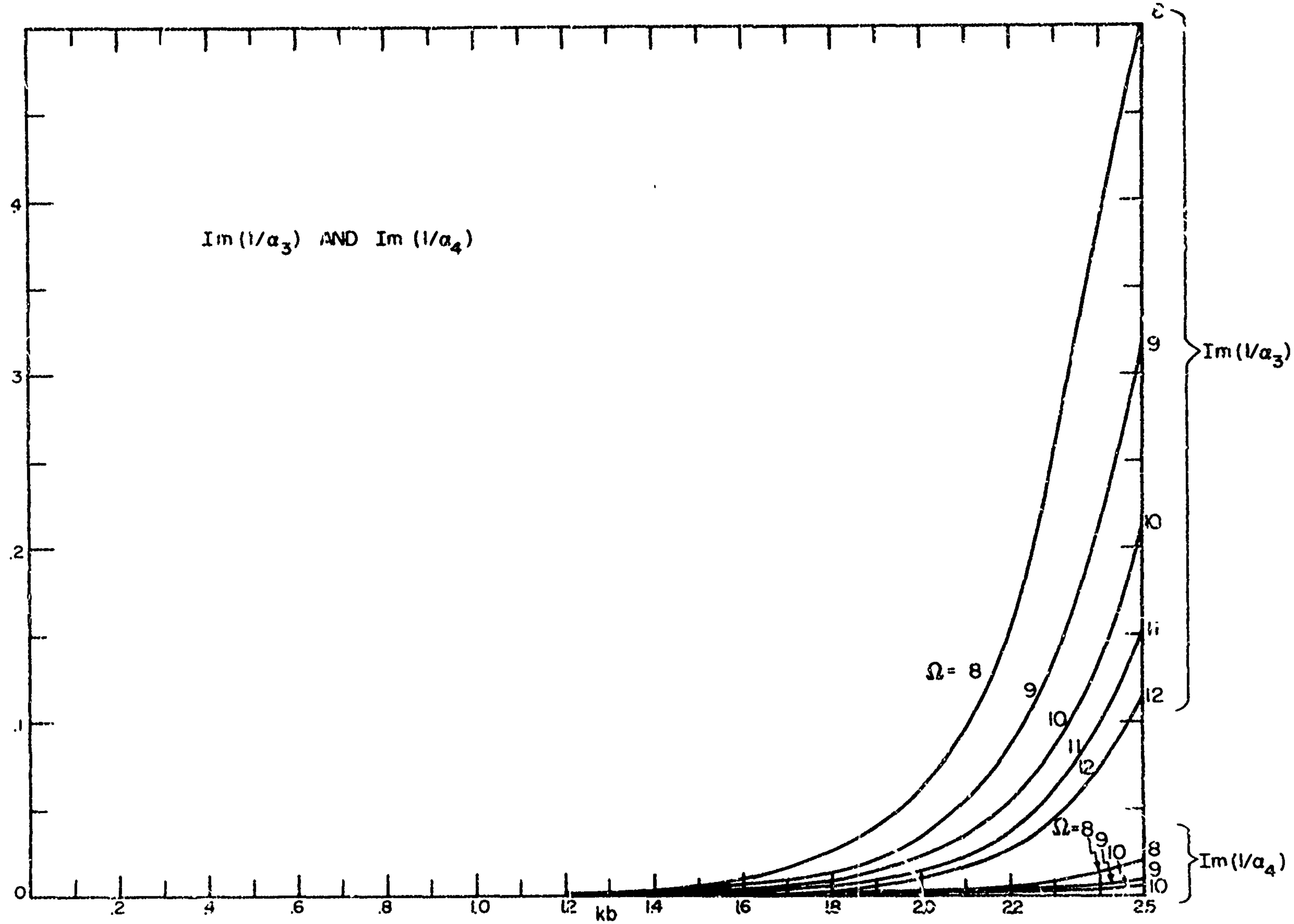
Im(1/α₃) AND Im(1/α₄)
Ω = 8
9
10
11
12
Im(1/α₃)
Im(1/α₄)
kb
0
.1
.2
3
4
.2
.4
.6
.8
1.0
1.2
1.4
1.6
1.8
2.0
2.2
2.5

FIG. C8

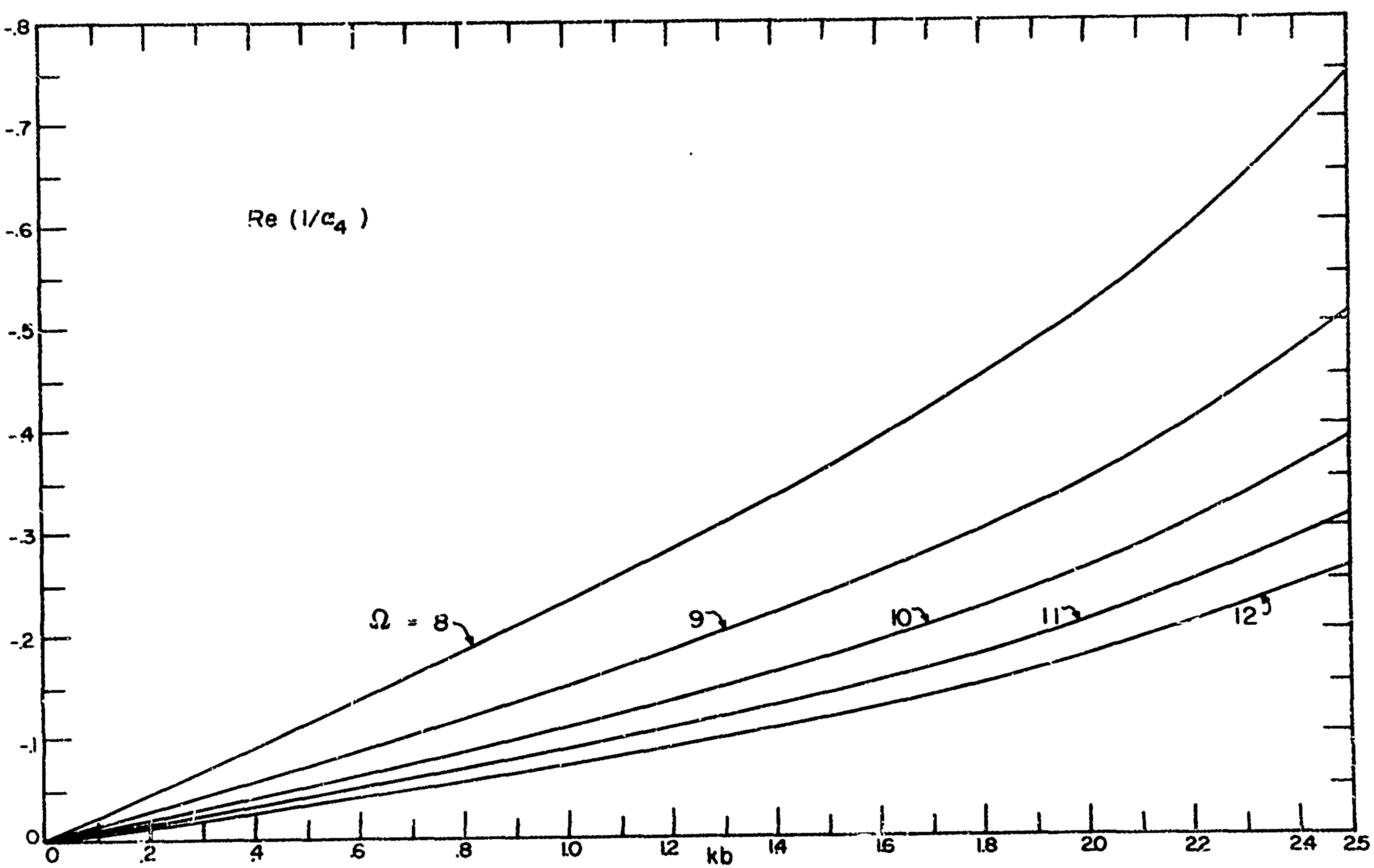

FIG. c9

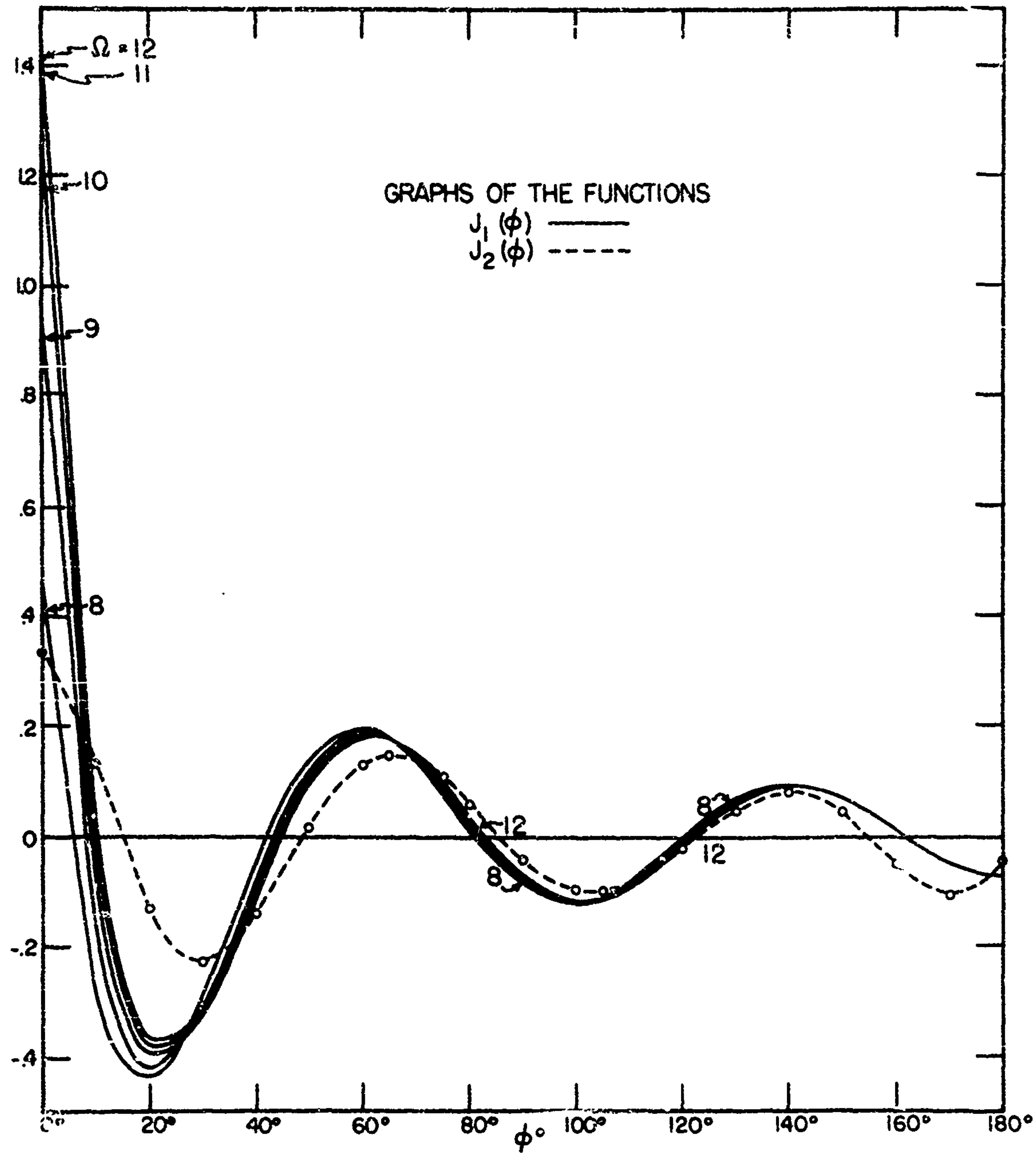
GRAPHS OF THE FUNCTIONS
$J_1(\phi)$
$J_2(\phi)$
$\Omega = 12$
11
10
9
8
12
8
8
12
1.4
1.2
1.0
.8
.6
.4
.2
0
-.2
-.4
0°
20°
40°
60°
80°
$\phi°$
100°
120°
140°
160°
180°

FIG. 10

DISTRIBUTION LIST

Technical Reports

	Chief of Naval Research Department of the Navy Washington 25, C. C.	
2		427
1		460
1		421
6	Director (Code 5250) Naval Research Laboratory Washington 25, D. C.	
2	Commanding Officer Office of Naval Research Branch Office 150 Causeway Street Boston, Massachusetts	
1	Commanding Officer Officer of Naval Research Branch Office 1000 Geary Street San Francisco 9, California	
1	Commanding Officer Office of Naval Research Branch Office 1030 E. Green Street Pasadena, California	
1	Commanding Officer Office of Naval Research Branch Office The John Crerar Library Building 86 East Randolph Street Chicago 1, Illinois	
1	Commanding Officer Office of Naval Research Branch Office 346 Broadway New York 13, New York	
3	Officer-in-Charge Office of Naval Research Navy No. 100 Fleet Post Office New York, New York	
	Chief, Bureau of Ordnance Navy Department Washington 25, D. C.	
1		Re4-1
1		AD-3

Technical Reports

	Chief, Bureau of Aeronautics Navy Department Washington 25, D. C.
1	EL-1
1	EL-4
2	Chief, Bureau of Ships (810) Navy Department Washington 25, D. C.
1	Chief of Naval Operations Navy Department Washington 25, D. C.
1	Op-413
1	Op-20
1	Op-32
1	Director Naval Ordnance Laboratory White Oak, Maryland
2	Commander U. S. Naval Electronics Laboratory San Diego, California
1	Commander(AAEL) Naval Air Development Center Johnsville, Pennsylvania
1	Librarian U. S. Naval Post Graduate School Monterey, California
50	Transportation Officer Building 151 Squier Signal Laboratory Fort Monmouth, New Jersey Attn: Director of Research
	Commanding General Air Research and Development Command Post Office Box 1395 Baltimore 3, Maryland
3	RDTRRP
2	RDDDE
1	Commanding General(WCRR) Wright Air Development Center Wright-Patterson Air Force Base, Ohio

Technical Reports

	Commanding General Wright Air Development Center Wright-Patterson Air Force Base, Ohio
1	WCRRH
2	WCLR
1	WCLRR
2	Technical Library
2	Commander Wright Air Development Center Attn: WCREO Wright-Patterson Air Force Base, Ohio
	Commanding General Rome Air Development Center Griffiss Air Force Base Rome, New York
1	RCREC-4C
1	RCR-1
2	RCRW
	Commanding General Air Force Cambridge Research Center 230 Albany Street Cambridge 39, Massachusetts
6	CRR
1	Technical Library
2	Director Air University Library Maxwell Air Force Base, Alabama
1	Commander Patrick Air Force Base Cocoa, Florida
1	Chief, European Office Air Research and Development Command Shell Building 60 Rue Ravenstein Brussels, Belgium
1	U. S. Coast Guard (EEE) 1300 E Street, N. W. Washington, D. C.
1	Assistant Secretary of Defense (Research and Development Research and Development Board Department of Defense Washington 25, D. C.

Technical Reports

5	Armed Services Technical Information Agency Document Service Center Knott Building Dayton 2, Ohio
1	Office of Technical Services Department of Commerce Washington 25, D. C.
1	Commanding Officer and Director U. S. Underwater Sound Laboratory New London, Connecticut
1	Federal Telecommunications Laboratories, Inc. Technical Library 500 Washington Avenue Nutley, New Jersey
1	Librarian Radio Corporation of America RCA Laboratories Princeton, New Jersey
1	Sperry Gyroscope Company Engineering Librarian Great Neck, L. I., New York
1	Watson Laboratories Library Red Bank, New Jersey
1	Professor E. Weber Polytechnic Institute of Brooklyn 9? Livingston Street Brooklyn 2, New York
1	University of California Department of Electrical Engineering Berkeley, California
1	Dr. E. T. Booth Hudson Laboratories 145 Palisade Street Dobbs Ferry, New York
1	Cornell University Department of Electrical Engineering Ithaca, New York
1	University of Illinois Department of Electrical Engineering Urbana, Illinois

Technical Reports

1	Johns Hopkins University Applied Physics Laboratory Silver Spring, Maryland
1	Professor A. von Hippel Massachusetts Institute of Technology Research Laboratory for Insulation Research Cambridge, Massachusetts
1	Director Lincoln Laboratory Massachusetts Institute of Technology Cambridge 39, Massachusetts
1	Mr. A. D. Bedrosian Room 22A-209 Signal Corps Liaison Office Massachusetts Institute of Technology Cambridge, Massachusetts
1	Mr. Hewitt Massachusetts Institute of Technology Document Room Research Laboratory of Electronics Cambridge, Massachusetts
1	Stanford University Electronics Research Laboratory Stanford, California
1	Professor A. W. Straiton University of Texas Department of Electrical Engineering Austin 12, Texas
1	Yale University Department of Electrical Engineering New Haven, Connecticut
1	Mr. James F. Trosch, Administrative Aide Columbia Radiation Laboratory Columbia University 538 West 120th Street New York 27, New York
1	Dr. J.V.N. Granger Stanford Research Institute Stanford, California
1	Library Central Radio Propagation Laboratory National Bureau of Standards Boulder, Colorado

Technical Reports

1	Library of the College of Engineering New York University University Heights Library University Heights 33, New York
1	Documents and Research Information Section Raytheon Manufacturing Company Engineering Equipment Division 148 California Street Newton 58, Massachusetts
1	Professor Henry G. Bocker School of Electrical Engineering Cornell University Ithaca, New York
1	M. A. Krivanich, Technical Advisor to Deputy Chief Ballistics Research Laboratory White Sands Annex White Sands P.G., New Mexico
1	Doris P. Baster Head, Document Section Technical Information Division Naval Research Laboratory Washington 25, D. C.
1	Dr. C. H. Papas Department of Electrical Engineering California Institute of Technology Pasadena, California
1	Airborne Instrument Laboratory Mineola New York
1	Radiation Laboratory Johns Hopkins University 1315 St. Paul Street Baltimore 2, Maryland
1	Mr. Robert Turner General Electric Company Advanced Electronics Center Cornell University Ithaca, New York

Technical Reports

1	Acquisitions Officer ASTIA Reference Center The Library of Congress Washington 25, D. C.
1	Librarian National Bureau of Standards Library Connecticut Avenue and Van Ness Street, N. E. Washington 25, D. C.
1	Secretary Working Group on Semiconductor Devices, AGET 346 Broadway, 8th Floor New York 13, N. Y.
1	Professor R. E. Norberg Washington University St. Louis, Missouri